Clinical and Experimental Allergy, 37, 735–742

ORIGINAL PAPER

Overexpression of suppressor of cytokine signalling-5 augments eosinophilic airway inflammation in mice

M. Ohshima*†, A. Yokoyama†, H. Ohnishi†, H. Hamada*, N. Kohno†, J. Higaki* and T. Naka‡

*Internal Medicine II, Ehime University School of Medicine, Tohon, Ehime, Japan, †Molecular and Internal Medicine, Graduate School of Biomedical Sciences, Hiroshima University, Hiroshima, Japan and ‡Department of Molecular Medicine, Osaka University Graduate School of Medicine, Osaka, Japan

Clinical and Experimental Allergy

Summary

Background Enhanced expression of the suppressor of cytokine signalling (SOCS)-5 might be of therapeutic benefit for T-helper type 2 (Th2) dominant diseases, as its expression is reported to result in a reduction of Th2 differentiation *in vitro* due to the inhibition of IL-4 signalling.

Objective To investigate the regulatory role of SOCS-5 *in vivo*, we explored the phenotype of an experimental asthma model developed in SOCS-5 transgenic (Tg) mice.

Methods The SOCS-5 Tg mice or wild-type (WT) mice were sensitized and repeatedly challenged with ovalbumin (OVA). We examined bronchoalveolar lavage fluid (BALF), lung specimens, and airway hyperresponsiveness (AHR) to methacholine.

Results The production of IFN-γ by $CD4^+$ T cells from unprimed SOCS-5 Tg mice was significantly increased in comparison with unprimed wild-type mice, indicating that SOCS-5 Tg mice have a Th1-polarizing condition under natural conditions. However, in an asthma model, significantly more eosinophils in the airways and higher levels of IL-5 and IL-13 in BALF were observed in the SOCS-5 Tg than the wild-type mice. AHR in the asthma model of SOCS-5 Tg was also more enhanced than that of wild-type mice. OVA-stimulated $CD4^+$ T cells from the primed SOCS-5 Tg mice produced significantly more IL-5 and IL-13 than $CD4^+$ T cells from wild-type mice.

Conclusion Our results demonstrate that the overexpression of SOCS-5 does not inhibit Th2 response, but rather augments the phenotype of the asthma model *in vivo*. This finding throws into question the therapeutic utility of using enhancement of SOCS-5 expression for Th2-dominant disease.

Correspondence:
Dr Akihito Yokoyama, Department of Molecular and Internal Medicine, Graduate School of Biomedical Sciences, Hiroshima University, 1-2-3 Kasumi, Minami-ku, Hiroshima 734-8551, Japan.
E-mail: yokoyan@hiroshima-u.ac.jp

Keywords asthma, $CD4^+$ T cells, cytokines, epidermal growth factor, rodent
Submitted 28 December 2006; revised 20 January 2007; accepted 23 February 2007

Introduction

Bronchial asthma is an immune-mediated disorder characterized by airway hyperresponsiveness (AHR) and eosinophilic airway inflammation. T-helper type 2 (Th2) cells are dominant in the airways and Th2 cytokines such as IL-4, IL-5 and IL-13 play a pivotal role in the pathophysiology of asthma [1–5]. Genetic and environmental factors influence the development of Th1 or Th2 cells [6]. The direction of Th cell differentiation is determined by the cytokine microenvironment at the site of the initial antigenic activation. The presence of IL-4 favours Th2 cell development, whereas the presence of IL-12 induces polarization to Th1 cells [6].

Recent studies indicate that suppressor of cytokine signalling (SOCS), which is a family of molecules that act as negative regulators for cytokine signalling, has an important role in the differentiation of Th1 and Th2 cells [7–10]. The SOCS proteins are a family of eight members (CIS and SOCS-1 to SOCS-7). Among the SOCS proteins, SOCS-3 is preferentially expressed in Th2 cells and has an important role in regulating the onset and maintenance of Th2-mediated allergic immune disease [11]. On the other hand, SOCS-5 is preferentially expressed in Th1 cells and its expression can result in a reduction of Th2 differentiation as a consequence of the inhibition of IL-4 signalling [12]. Like SOCS-5, SOCS-1 and SOCS-2 are also reported to be expressed primarily in Th1 cells [13]. *In vitro* differentiation assays with $CD4^+$ T cells from SOCS-3 or SOCS-5 transgenic (Tg) mice have revealed that SOCS-3 overexpression favours Th2 differentiation, whereas SOCS-5 overexpression favours Th1 differentiation [11, 12].

It is suggested that enhancement of the expression of SOCS-5 in $CD4^+$ T cells might be a useful therapeutic approach to Th2-dominant diseases [12, 14]. In fact, transfer of primed $CD4^+$ T cells *constitutively* expressing SOCS-5 along with eye drop challenges in a murine allergic conjunctivitis model resulted in attenuated eosinophilic inflammation with enhanced IFN-γ and decreased IL-13 production [14]. However, it should be noted that SOCS-5 appears to be dispensable for the development of Th1 responses *in vivo*, as demonstrated by use of the SOCS-5 knockout mice [15]. SOCS-5-deficient $CD4^+$ T cells can differentiate into either Th1 or Th2 cells with the same efficiency [15]. This may be due to functional redundancy between SOCS family proteins. In particular, SOCS-4 and SOCS-5 share significant homology and therefore may have overlapping functions in the regulation of differentiation of $CD4^+$ T cells.

To define the role of SOCS-5 in a representative instance of Th2-dominant allergic asthma *in vivo*, we explored the phenotype of a typical ovalbumin (OVA)-primed and a challenged murine asthma model by using SOCS-5 Tg mice. The above information suggests amelioration of the Th2-driven phenotype in SOCS-5 Tg mice due to an inhibition of the Th2 differentiation induced by the constitutive expression of SOCS-5 in $CD4^+$ T cells. Unexpectedly, however, we in fact observed an exaggerated phenotype with characteristics such as increased eosinophilic inflammation and AHR in the SOCS-5 Tg mice.

Materials and methods

Animals

The specific pathogen-free C57BL/6 (B6) mice were obtained from Charles River Laboratories (Kanagawa, Japan) as were the wild-type (WT) mice. Chicken β-actin promoter-controlled Tg mice were established as reported elsewhere [12]. All experiments were performed according to an institutional guideline. The committee on Animal Welfare of Ehime University approved the protocols used in this study.

Mouse sensitization and challenge

The methods for a typical OVA-induced murine asthma model were described previously [16–18]. Briefly, 6-week-old WT and SOCS-5 Tg mice were primed intraperitoneally with 10 μg OVA (Grade V; Sigma Chemical Co., St Louis, MO, USA) and 20 mg aluminium hydroxide in 0.2 mL phosphate-buffered saline (PBS, pH 7.4) once per week for 2 weeks (weaker inflammation model) or 3 weeks (stronger model). Twenty-four hours after the last injection, the primed mice were individually placed in a mouse aerosol delivery system (Central Scientific Commerce Inc., Tokyo, Japan) and exposed to 5% aerosolized (DeVilbliss Co., Somerset, PA, USA) OVA dissolved in saline, delivered by a DeVilbiss 646 nebulizer pressed air at 5 L/min for 20 min. Challenge was carried out once a day for 2 (weaker inflammation model) or 6 (stronger model) consecutive days. For the negative control group, PBS alone was used for priming and exposure instead of OVA.

Real-time quantitative reverse transcriptase-polymerase chain reaction

Total RNA was isolated from spleen and lung cells by using the RNeasy kit (Qiagen, Tokyo, Japan) according to the manufacturer's instructions. The AMV reverse transcriptase first-strand cDNA Synthesis Kit (Life Sciences Inc., St Petersburg, FL, USA) was used to synthesize cDNA for reverse transcription of 1 μg of RNA per sample, and a negative control with no enzyme was included for all samples. Quantitative RT-PCR was performed with a Lightcycler (Roche Diagnostics, Castle Hill, Australia) with the forward and reverse mouse primers for glyceraldehyde-3-phosphate dehydrogenase (GAPDH) (F: 5′-TGAACGGGAAGCTCACTGG-3′; R:5′-TCCACCACCCT GTTGCTGTA-3′) and SOCS-5 (F:5′-ACTTTCCCTTTCAGC CTGC-3′, R:5′-TCTAACCAGCGAACCCTAACT-3′). Cycling conditions consisted of initial denaturation (95 °C for 10 min), followed by PCR cycles with a transition rate of 20 °C/s and a single-fluorescence-measurement melting curve program (70–95 °C), at a heating rate of 0.1 °C/s and continuous fluorescence measurement), followed by cooling to 40 °C in the final step. All PCRs were performed with a QuantiTect SYBR Green PCR kit (Qiagen). The specificity of the SYBR green reaction was assessed by melting point analysis and gel electrophoresis. SOCS-5 mRNA levels were quantified with standard curves by using Roche Molecular Biochemicals Lightcycler software (version 3.5) and are presented as arbitrary units standardized against GAPDH mRNA. Standard curves were generated by using dilutions of an oligonucleotide corresponding to the amplified fragments of GAPDH and SOCS-5. Poly$(A)^+$ mRNA was isolated from individual tissues.

Measurement of airway hyperresponsiveness

The airway response of freely moving mice to aerosolized methacholine (MCh) was measured 24 h after the final aerosol challenge (day 11 or 21) by whole-body plethysmography (Buxco, Troy, NY, USA), as described previously [16–18]. Before taking readings, the box was calibrated by a rapid injection of 100 mL air into the main chamber. Pressure differences between the main chamber containing the mouse and a reference chamber were recorded. Readings were obtained at baseline and after exposure to aerosolized PBS or MCh (6.25–50 mg/mL). Data were

averaged for 5 min, and expressed as the 'enhanced pause' (Penh): $Penh = [(T_e - T_r)/T_r] \times (PEP/PIP)$, where T_e is the expiratory time (s), T_r is the relaxation time (time of the pressure decay to 36% of total box pressure during expiration), PEP is the peak expiratory pressure (mL/s), and PIP is the peak inspiratory pressure (mL/s). Results are expressed as the percentage increase of Penh following challenge with each concentration of MCh, where the baseline Penh (after PBS challenge) is expressed as 100%.

Bronchoalveolar lavage and histologic examination

Forty-eight hours after the final challenge (day 12 or 22), mice were killed by cervical dislocation under anaesthesia. Bronchoalveolar lavage fluid (BALF) was obtained by the slow injection of PBS 0.5 mL into the trachea using a cannula three times (a total of 1.5 mL). This procedure always yielded > 80% recovery of the infused fluid. The total number of cells in BALF was counted by a haemocytometer. A differential count was made by cytospin preparations (150 g, 2 min, at room temperature). The cells were fixed and stained with May–Giemsa. Differential counts of at least 300 cells were performed using standard morphological criteria to identify eosinophils. The absolute number of eosinophils in BALF was then calculated. The BALF was stored at − 80 °C until use. IL-5, IL-13 and IFN-γ ELISA kits were purchased from Endogen (Rockford, IL, USA) or R&D systems (Minneapolis, MN, USA). The concentrations of these cytokines in BALF were assayed according to the procedures recommended by the manufacturers. The limit of detection was 1.5 pg/mL for IL-13 and IFN-γ and 10 pg/mL for IL-5.

Following BAL, lungs were perfused with PBS (10 mL) through the right ventricle. Then the lungs were removed and fixed with 4% paraformaldehyde. The specimens were cut (vertically to the lower lobe bronchus) into 2 μm slices, placed onto slides and stained with haematoxylin eosin or alcian blue and periodic acid-Schiff (AB/PAS), according to a standard protocol. The numbers of goblet cells (AB/PAS-positive cells) and eosinophils were counted using an image analysis system. The stained slides were examined with a light microscope (AX 80; Olympus, Tokyo, Japan), connected to a digital camera (HC-300; Fuji Film, Tokyo, Japan) and an image capture board (Photograb-300, Fuji Film). Images of the intrapulmonary airway epithelium (large airway in the specimen) were recorded from five consecutive high-power fields at × 400. Analysis was performed on a Power Macintosh G4 computer (Apple Computer, Cupertino, CA, USA) using the public domain NIH Image program (developed at the US National Institutes of Health and available on the internet at http://rsb.info.nih.gov/nih-image/). Data are expressed as the number of cells per millimeter of the subepithelial basement membrane.

Cytokine production of splenic $CD4^+$ T cells

The spleens of mice were removed aseptically and pressed through a wire mesh screen to separate cells. The splenic mononuclear cells (SMNC) were purified by a density gradient method using Lympholyte-M (Cedarlane Labs, Burlington, ON, Canada). $CD4^+$ T cells were separated from SMNCs using MACS CD4 (L3T4) microBeads (conjugated to monoclonal rat anti-mouse CD4 antibodies) and Mini-MACS MS Separation Columns (Miltenyi Biotec, Auburn, CA, USA). Then the cells were suspended in RPMI 1640 medium supplemented with 10% heat-inactivated fetal calf serum (Gibco, Carlsbad, CA, USA), 100 U/mL penicillin G, 100 μg/mL streptomycin, 50 μmol/L 2-mercaptoethanol (2-ME; Sigma), and 10 mmol/L *N*-2-hydroxyethylpiperazine-*N*-2-ethanesulphonic acid (HEPES) (Sigma). Cells were seeded at 2×10^6 cells/mL on 96-well flat-bottomed plates for collecting the supernatant. For the stimulation of the cells, 1 μg/mL concanavalin A (Con A) and 1 mg/mL OVA were added to the culture wells. The cells were cultured at 37 °C in a humidified incubator in a 5% CO_2 atmosphere for 48 h. The supernatant was then collected and stored at − 80 °C until use.

Statistical analysis

Data are expressed as the mean ± SE. The significance of difference between the data from each group was determined using Student's *t*-test following one-way analysis of variance (ANOVA) when applicable. Mann–Whitney *U*-test was applied for the comparison of cytokine concentrations. A *P*-value of < 0.05 was considered statistically significant.

Results

As shown in Fig. 1a, real-time quantitative RT-PCR analysis for SOCS-5 mRNA revealed an approximately two times higher expression of SOCS-5 in both the spleen and lung from SOCS-5 Tg mice than WT mice. A previous study showed that a relatively small increase of SOCS-5 expression in T cells, i.e., on the order of twofold or lower, induced skewed differentiation towards Th1 [12]. In accordance with this finding, purified $CD4^+$ T cells from SOCS-5 Tg mice spontaneously secreted eight times more IFN-γ than $CD4^+$ T cells from WT mice (Fig. 1b). Secretion of IFN-γ in response to Con A from SOCS-5 Tg $CD4^+$ T cells was also >3 times more than that from WT $CD4^+$ T cells (Fig. 1b).

By using such SOCS-5 Tg mice, we were able to compare the phenotype of an experimental asthma model between SOCS-5 Tg and WT mice. At first, we tried our usual asthma model (three times sensitization and six challenges, a stronger inflammation model). The number of total cells and eosinophils in BALF were increased in

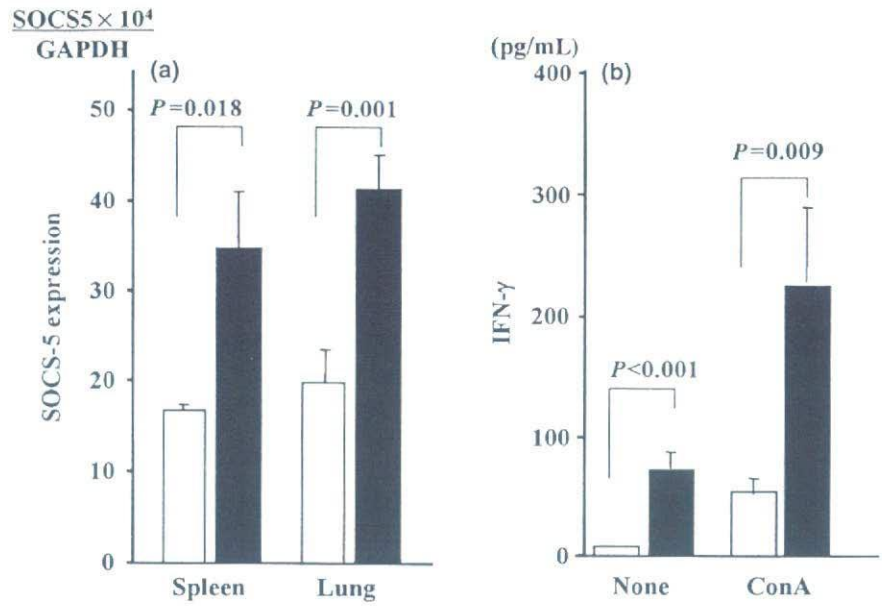

Fig. 1. Quantitative RT-PCR for suppressor of cytokine signalling (SOCS-5) mRNA (a) and production of IFN-γ from $CD4^+$ T cells (b). Expression of SOCS-5 is approximately twofold higher in SOCS-5 transgenic (Tg) mice (closed column; $n = 10$) in comparison with wild-type (WT) mice (open column; $n = 8$). Production of IFN-γ in purified $CD4^+$ T cells from SOCS-5 Tg mice is eight times (spontaneous) or >3 times (stimulation with concanavalin A) more than that from WT mice. Data are shown as mean ± SE.

this model, but were not significantly different between SOCS-5 Tg and WT mice (data not shown). Furthermore, AHR was obvious in both models but was also not significantly different between SOCS-5 Tg and WT mice (data not shown). SOCS-5 mRNA expression in both the lung and spleen from SOCS-5 Tg mice asthma model was twice as much as the expression in WT mice. According to a previous report, T cells from SOCS-5 Tg mice exhibit a reduction in Th2 development to half that of control WT mice [8]. Therefore, we considered that the stronger stimulation may negate the inhibitory effect of SOCS-5 on the development of Th2 cells.

Therefore, we decided to examine a milder asthma model (two times sensitization and two challenges; weaker inflammation model). In this model, total cell counts and eosinophils in BALF were less than one half those of the stronger inflammation model. Unexpectedly to us, however, in this weaker model, the total cell counts and number of eosinophils in BALF from the SOCS-5 Tg mice were markedly higher than those in WT mice (Fig. 2a). The eosinophils in BALF from the SOCS-5 Tg mice were three times as much as those in the WT mice. However, the number of neutrophils or macrophages in BALF was not significantly different between the asthma model mice of SOCS-5 Tg and WT mice. The AHR of the SOCS-5 Tg mice was also significantly more enhanced than that of WT mice (Fig. 2b). Histological examination revealed similar inflammatory changes such as epithelial cell damage with goblet cell hyperplasia, and eosinophil-dominant cellular infiltration, particularly in the bronchovascular bundles, but the degree of these changes was different between the SOCS-5 Tg and WT mice (Fig. 3). Submucosal eosinophilic infiltration was observed more prominently in the asthma model of SOCS-5 Tg mice than that of WT mice (Figs 3a, c and e). The number of AB/PAS-staining goblet cells in SOCS-5 Tg mice was significantly increased compared with those in WT mice (Figs 3b, d and e).

These observations that a more pronounced asthmatic phenotype was developed in SOCS-5 Tg than WT mice were supported by the cytokine levels in BALF (Fig. 4) and the culture supernatant from OVA-stimulated $CD4^+$ T cells (Fig. 5). Comparable amounts of IFN-γ and IL-5 in BALF were detected in both asthma models but these were significantly higher in SOCS-5 Tg than WT mice (Fig. 4). The level of IL-13 in BALF was much higher in the SOCS-5 Tg than the WT mice. It should be noted that the level of IFN-γ but not IL-5 or IL-13 in BALF was increased almost threefold in the PBS-primed and -challenged SOCS-5 Tg mice in comparison with the WT mice. Furthermore, the production of IFN-γ from OVA-stimulated $CD4^+$ T cells in SOCS-5 Tg mice was significantly higher compared with the WT mice. Production of the Th2 cytokines IL-5 and IL-13 were significantly higher in the asthma model SOCS-5 Tg mice than the WT mice (Fig. 5).

Discussion

In the present study, we demonstrated that overexpression of SOCS-5 does not inhibit Th2-dominant disease, and rather augments eosinophilic inflammation *in vivo*. SOCS-5 inhibits IL-4 signalling via binding to the IL-4 receptor and inhibition of Jak 1-STAT 6 activation pathways [12]. This

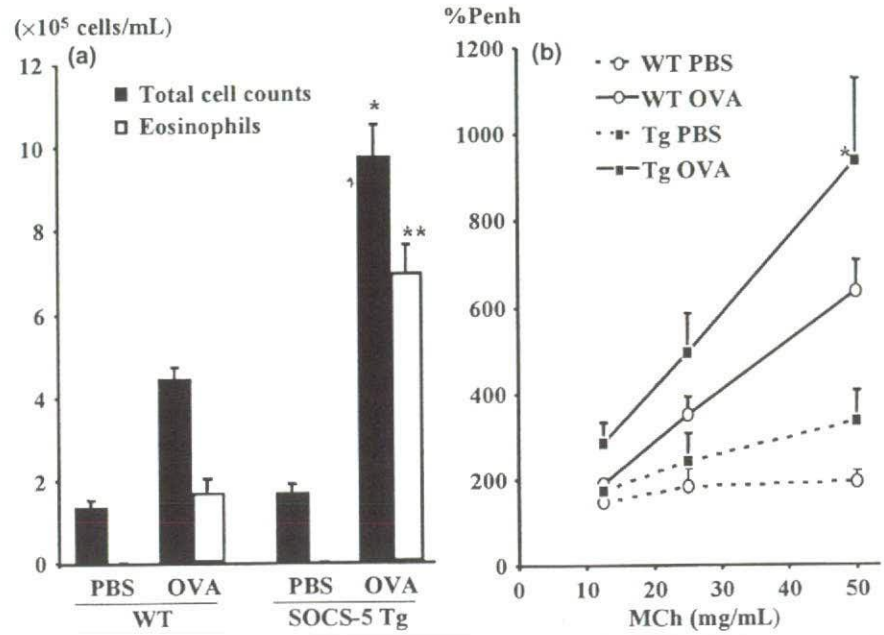

Fig. 2. Analysis of cells in bronchoalveolar lavage fluid (a) and airway responses to aerosolized methacholine (MCh) (b). (a) Total cell (closed column) and eosinophil (open column) counts are significantly increased in ovalbumin (OVA)-sensitized and -challenged suppressor of cytokine signalling (SOCS-5) transgenic (Tg) mice in comparison with OVA-sensitized and -challenged wild-type (WT) mice. (b) Airway hyperresponsiveness (AHR) was observed in OVA-sensitized and -challenged mice (lines) but not phosphate-buffered saline-challenged mice (dotted lines). The degree of AHR was significantly increased in SOCS-5 Tg mice (closed square) compared with WT mice (open circle). Data are shown as mean ± SE ($n = 8$–10). $^{*}P < 0.05$, $^{**}P < 0.005$, when compared with WT mice.

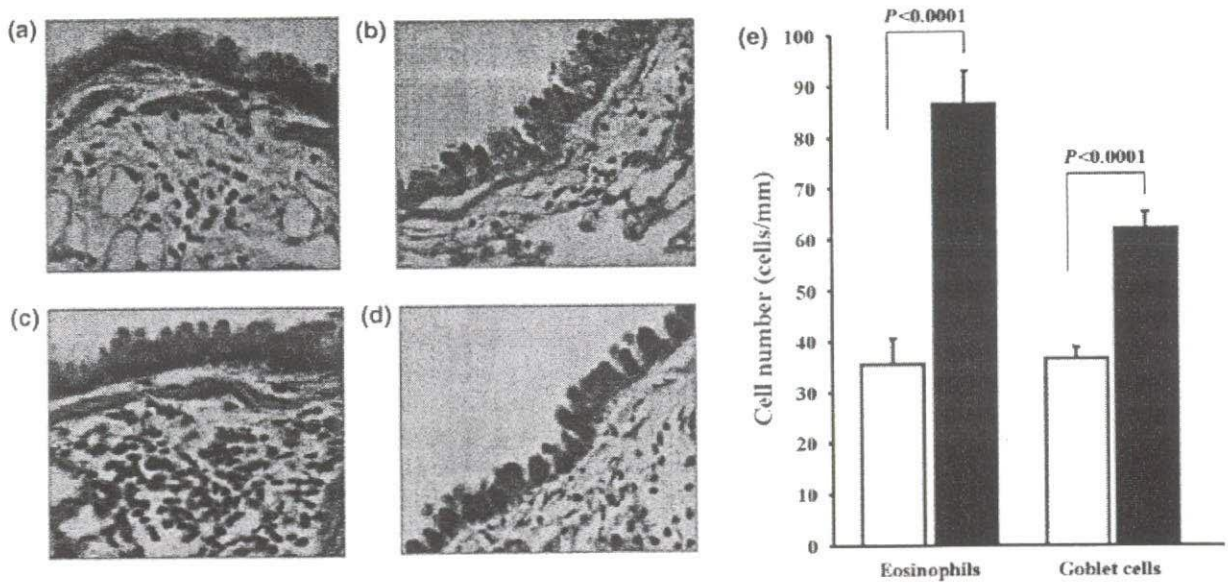

Fig. 3. Representative photos of the lungs from ovalbumin (OVA)-sensitized and -challenged mice (a–d) and morphometric analysis (e). Lung specimens of asthma model mice in wild-type (WT) (a, b) or suppressor of cytokine signalling (SOCS-5) transgenic (Tg) (c, d) were stained with haematoxylin and eosin (a, c) and alcian blue and periodic acid-Schiff (b, d). The number of eosinophils in subepithelium and number of goblet cells in the airway epithelium were significantly increased in SOCS-5 Tg mice (closed column) in comparison with WT mice (open column) (e). Original magnification ×200.

effect should be accompanied by inhibition of differentiation of Th2 cells, as IL-4 signalling is crucial for Th2 differentiation [6]. In fact, overexpression of SOCS-5 in T cells induced a Th1-skewing condition, as described previously [12]. The present study confirmed this observation, as evidenced by the exaggerated IFN-γ production from Con A-stimulated $CD4^{+}$ T cells (Fig. 1). Even under such conditions, eosinophilic inflammation and AHR in the

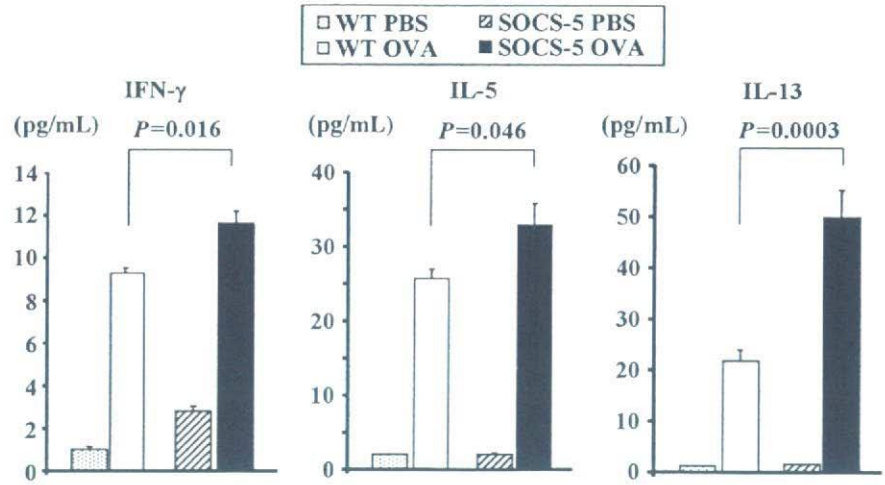

Fig. 4. Cytokine profiles in bronchoalveolar lavage fluid. Levels of IFN-γ, IL-5 and IL-13 were significantly increased in the asthma model of the suppressor of cytokine signalling transgenic mice in comparison with wild-type mice. Data are expressed as mean ± SE ($n = 8$).

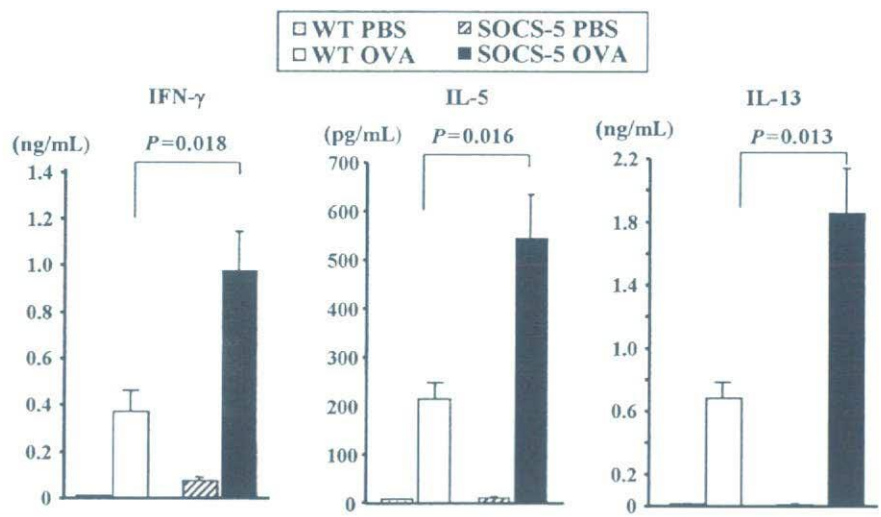

Fig. 5. Production of IFN-γ, IL-5 and IL-13 by $CD4^+$ T cells. $CD4^+$ T cells were purified from spleen cells of each group of mice and stimulated by ovalbumin for 48 h. Production of IFN-γ, IL-5 and IL-13 were significantly increased in the suppressor of cytokine signalling transgenic mice in comparison with wild type mice. Data are expressed as mean ± SE ($n = 6$).

SOCS-5 Tg mice asthma model mice were more prominent than those observed in WT mice. The lungs from the asthma model of SOCS-5 Tg mice exhibited a markedly increased number of eosinophils and goblet cells in the airways. Furthermore, OVA-stimulated $CD4^+$ T cells from SOCS-5 Tg mice produced significantly more cytokines (not only Th1 but also Th2) compared with those from the WT mice. These observations suggest that overexpression of SOCS-5 does not inhibit the development of Th2 response, and therefore the implication is that the strategy of increasing the expression of SOCS-5 would not be beneficial for the treatment of allergic diseases.

This study indicates that a Th1 dominant state may augment the allergic phenotype in asthma model mice. In the murine asthma model, expression of IFN-γ is known to be in the early stage of inflammation [19, 20]. Randolph et al. [19] demonstrated that Th1 cells predominate early in the development of eosinophilic inflammation, and Th2 cells predominate later in the OVA-induced murine asthma model. They also demonstrated cooperation between Th1 and Th2 cells: Th2 cells require additional signals for effective recruitment to the airways, and Th1 cells are able to provide these extra signals [21]. Although exogenous or systemic IFN-γ is known to ameliorate established eosinophilic airway inflammation, endogenous or lung-specific expression of IFN-γ plays a role in an optimal Th2-driven airway inflammation [20, 22, 23]. The relative contribution of IFN-γ with such pleiotropic activities may be associated with the obvious effects of SOCS-5 in the milder asthma model. At first, we used a more severe asthma model with three times sensitization and six times challenges. In these mice, eosinophilic inflammation and airway

responsiveness to the non-specific bronchoconstrictor MCh did not exhibit any difference between the SOCS-5 Tg and WT mice.

This study also suggests the Th1-dominant state is not inhibitable by the development of Th2 dominant disease *in vivo*. As described previously, the development of a Th1- or Th2-based response is considered to be alternative and to depend on the cytokines present in the induction microenvironment [6]. It has been considered that the induction of IFN-γ and Th1-type immunity, which are thought to be important against infectious organisms, would counter-regulate the development of Th2 responses. These hypothetical accounts provide the background for the 'hygiene hypothesis'. However, the increasing prevalence of Th1-dominant disorders in parallel with the asthma epidemic suggests that the induction of Th1-driven immunity cannot explain the protection mechanism [24]. Recent work has focused on the induction of regulatory cells that suppress both Th1- and Th2-type responses [25, 26]. This study also indicates that the ostensible counter-regulatory mechanism does not work *in vivo* and provides further evidence against the conventional hygiene hypothesis.

It is noteworthy that goblet cell hyperplasia/metaplasia of airway epithelial cells was not inhibited but instead was rather increased in the asthma model of SOCS-5 Tg mice. SOCS-5 can associate with epidermal growth factor receptor (EGFR) and inhibit EGFR signalling via degradation of EGFR [27, 28]. Although the mechanisms for goblet cell hyperplasia are not fully understood, EGFR activation with subsequent signalling via EGFR tyrosine kinase and mitogen activated protein kinase appears to be a convergent pathway involved in the goblet cell hyperplasia induced by insults such as oxidative stress and Th2 cytokines [29–31]. Therefore, it would be reasonable to expect less goblet cell hyperplasia in SOCS-5 Tg mice. However, our results suggest that a small increase of SOCS-5 expression (e.g. twice) may not affect EGFR signalling, or EGF signalling may not be involved in the mechanism of goblet cell hyperplasia/metaplasia, at least in an OVA-induced usual asthma model.

In conclusion, we have demonstrated that the overexpression of SOCS-5 does not inhibit Th2 response, and appears to augment eosinophilic inflammation, including goblet cell hyperplasia, in *vivo*. Therefore, these results suggest that SOCS-5 is not a good target for therapeutic intervention in allergic asthma.

Acknowledgements

The authors have no financial conflict of interest. This work was supported by a Grant in Aid for Scientific Research of the Ministry of Education, Culture, Sports, Science and Technology Japan.

References

1 Busse WW, Lemanske RF Jr. Asthma. *N Engl J Med* 2001; 344:350–62.
2 Larche M, Robinson DS, Kay AB. The role of T lymphocytes in the pathogenesis of asthma. *J Allergy Clin Immunol* 2003; 111:450–63.
3 Zimmermann N, Hershey GK, Foster PS, Rothenberg ME. Chemokines in asthma: cooperative interaction between chemokines and IL-13. *J Allergy Clin Immunol* 2003; 111: 227–42.
4 Katayama H, Yokoyama A, Kohno N *et al.* Production of eosinophilic chemokines by normal pleural mesothelial cells. *Am J Respir Cell Mol Biol* 2002; 26:398–403.
5 Tanaka H, Komai M, Nagao K *et al.* Role of interleukin-5 and eosinophils in allergen-induced airway remodeling in mice. *Am J Respir Cell Mol Biol* 2004; 31:62–8.
6 Murphy KM, Reiner SL. The lineage decisions of helper T cells. *Nat Rev Immunol* 2002; 2:933–44.
7 Jiang H, Harris MB, Rothman P. IL-4/IL-13 signaling beyond JAK/STAT. *J Allergy Clin Immunol* 2000; 105:1063–70.
8 Alexander WS, Hilton DJ. The role of suppressors of cytokine signaling (SOCS) proteins in regulation of the immune response. *Annu Rev Immunol* 2004; 22:503–29.
9 Fujimoto M, Naka T. Regulation of cytokine signaling by SOCS family molecules. *Trends Immunol* 2003; 24:659–66.
10 Inoue H, Kubo M. SOCS proteins in T helper cell differentiation: implications for allergic disorders? *Expert Rev Mol Med* 2004; 6:1–11.
11 Seki Y, Inoue H, Nagata N *et al.* SOCS-3 regulates onset and maintenance of T(H)2-mediated allergic responses. *Nat Med* 2003; 9:1047–54.
12 Seki Y, Hayashi K, Matsumoto A *et al.* Expression of the suppressor of cytokine signaling-5 (SOCS5) negatively regulates IL-4-dependent STAT6 activation and Th2 differentiation. *Proc Natl Acad Sci USA* 2002; 99:13003–8.
13 Egwuagu CE, Yu CR, Zhang M, Mahdi RM, Kim SJ, Gery I. Suppressors of Cytokine signaling proteins are differentially expressed in Th1 and Th2 cells: Implications for Th cell lineage commitment and maintenance. *J Immunol* 2002; 168:3181–7.
14 Ozaki A, Seki Y, Fukushima A, Kubo M. The control of allergic conjunctivitis by suppressor of cytokine signaling (SOCS) 3 and SOCS-5 in a murine model. *J Immunol* 2005; 175:5489–97.
15 Brender C, Columbus R, Metcalf D *et al.* SOCS-5 is expressed in primary B and T lymphoid cells but is dispensable for lymphocyte production and function. *Mol Cell Biol* 2004; 24:6094–103.
16 Sakai K, Yokoyama A, Kohno N, Hiwada K. Effect of different sensitizing doses of antigen in a murine model of atopic asthma. *Clin Exp Immunol* 1999; 118:9–15.
17 Yokoyama A, Hamazaki T, Ohshita A *et al.* Effect of aerosolized docosahexaenoic acid in a mouse model of atopic asthma. *Int Arch Allergy Immunol* 2000; 123:327–32.
18 Sakai K, Yokoyama A, Kohno N, Hamada H, Hiwada K. Prolonged antigen exposure ameliorates airway inflammation but not remodeling in a mouse model of bronchial asthma. *Int Arch Allergy Immunol* 2001; 126:126–34.
19 Randolph DA, Carruthers CJ, Szabo SJ, Murphy KM, Chaplin DD. Modulation of airway inflammation by passive transfer of allergen-specific Th1 and Th2 cells in a mouse model of asthma. *J Immunol* 1999; 162:2375–83.

20 Koch M, Witzenrath M, Reuter C *et al.* Role of local pulmonary interferon gamma expression in murine allergic airway inflammation. *Am J Respir Cell Mol Biol* 2006; 35:211–9.
21 Randolph DA, Stephens R, Carruthers CJ, Chaplin DD. Cooperation between Th1 and Th2 cells in a murine model of eosinophilic airway inflammation. *J Clin Invest* 1999; 104:1021–9.
22 Nakajima H, Iwamoto I, Yoshida S. Aerosolized recombinant interferon-gamma prevents antigen-induced eosinophil recruitment in mouse trachea. *Am Rev Respir Dis* 1993; 148: 1102–4.
23 Hofstra CL, Van Ark I, Hofman G, Nijkamp FP, Jardieu PM, Van Oosterhout AJ. Differential effects of endogenous and exogenous interferon-gamma on immunoglobulin E, cellular infiltration, and airway responsiveness in a murine model of allergic asthma. *Am J Respir Cell Mol Biol* 1998; 19:826–35.
24 Bach JF. The effect of infections on susceptibility to autoimmune and allergic diseases. *N Engl J Med* 2002; 347:911–20.
25 Wills-Karp M, Santeliz J, Karp CL. The germless theory of allergic disease: revisiting the hygiene hypothesis. *Nat Rev Immunol* 2001; 1:69–75.
26 Prioult G, Nagler-Anderson C. Mucosal immunity and allergic responses: lack of regulation and/or lack of microbial stimulation? *Immunol Rev* 2005; 206:204–18.
27 Kario E, Marmor MD, Adamsky K *et al.* Suppressors of cytokine signaling 4 and 5 regulate epidermal growth factor receptor signaling. *J Biol Chem* 2005; 280:7038–48.
28 Nicholson SE, Metcalf D, Sprigg NS *et al.* Suppressor of cytokine signaling (SOCS)-5 is a potential negative regulator of epidermal growth factor signaling. *Proc Natl Acad Sci USA* 2005; 102:2328–33.
29 Takeyama K, Dabbagh K, Jeong Shim J, Dao-Pick T, Ueki IF, Nadel JA. Oxidative stress causes mucin synthesis via transactivation of epidermal growth factor receptor: role of neutrophils. *J Immunol* 2000; 164:1546–52.
30 Dabbagh K, Takeyama K, Lee HM, Ueki IF, Lausier JA, Nadel JA. IL-4 induces mucin gene expression and goblet cell metaplasia in vitro and in vivo. *J Immunol* 1999; 162:6233–7.
31 Casalino-Matsuda SM, Monzon ME, Forteza RM. Epidermal growth factor receptor activation by EGF mediates oxidant-induced goblet cell metaplasia in human airway epithelium. *Am J Respir Cell Mol Biol* 2006; 34:581–91.

●原 著

高度呼吸不全を呈した特発性肺線維症急性増悪における シベレスタットナトリウム使用成績と予後因子の検討

中村 万里　小倉 高志　宮沢 直幹　田川 暁大
小澤 聡子　綿貫 祐司　高橋 宏

要旨：2002年7月から2005年3月まで特発性肺線維症（IPF）急性増悪と診断，高度の呼吸不全を合併し人工呼吸器管理となり，好中球エラスターゼ阻害剤（シベレスタットナトリウム）を使用した10名の患者で，予後及び生存群と非生存群での予後因子の検討を行った．入院後180日目の生存で，生存群，非生存群でPaO_2/FiO_2（P/F），PEEP値，WBC数，CRP値の経時的変化，入院時血清中KL-6，SP-値を検討した．入院後180日目で，10名中4名が生存と良好な成績であった．生存群は入院後7日目でP/F，PEEP値，CRP値は改善（$p<0.05$），入院時の血清中のKL-6値，SP-D値は非生存群より低値であった（$p<0.05$）．シベレスタットナトリウムは高度呼吸不全を合併したIPF急性増悪の治療で効果を期待される可能性があると思われた．血清中KL-6及びSP-D値が予後予測因子として有用であると考えられた．

キーワード：特発性肺線維症，急性増悪，シベレスタットナトリウム，KL-6，SP-D
Idiopathic pulmonary fibrosis (IPF), Acute exacerbation, Sivelestat, KL-6, SP-D

緒　言

特発性間質性肺炎（IIPs）は，病理組織パターンによって臨床経過や治療反応性が異なる．その中でも，特発性肺線維症（IPF）は，急性に増悪，呼吸不全を合併，難治性で救命率は低い．IPFの急性増悪は，過去の報告によれば，初回増悪時の死亡率は約80％で，改善例でも平均6カ月で死亡するとされ，極めて予後不良な病態である[1)2)]．ともにステロイド剤や免疫抑制剤投与などの治療が行われるが治療成績は不良で確固とした治療法は確立されていない[1)3)]．わが国では急性肺障害（ALI/ARDS）に対し，2002年より好中球エラスターゼ阻害剤，シベレスタットナトリウム（商品名：エラスポール）が臨床使用可能となり，実際の臨床現場ではその効果が期待されている[4)]．IPF/UIPの血漿中の好中球エラスターゼは健常者と比較し上昇している．急性増悪時にはさらに上昇することが報告されており，IPF急性増悪時においてもシベレスタットナトリウムの臨床効果が期待される[5)6)]．今回我々は，高度呼吸不全をきたした特発性肺線維症急性増悪症例でシベレスタットナトリウム使用を行った10症例について，治療成績，予後，予後予測因子の検討を行った．

〒236-0051　横浜市金沢区富岡東6—16—1
神奈川県立循環器呼吸器病センター呼吸器科
（受付日平成18年3月7日）

研究対象，方法

対象は，2002年7月から2005年3月までに当センターへ入院，特発性肺線維症と診断され，高度呼吸不全をきたし人工呼吸器管理となった，シベレスタットナトリウムを使用した合計10名の患者で，男性8名，女性2名，年齢59歳～85歳（平均72±4.1歳）であった．特発性肺線維症（IPF）の診断は，入院時身体理学所見，入院時胸部X線所見，胸部CTの画像所見及び検査データ，病歴より日本呼吸器学会の特発性間質性肺炎の診断・治療ガイドライン[6)]及びAmerican Thoracic Societyの診断基準に従って行った．IPF急性増悪の診断は，厚労省の改定案によった．今回の検討の対象となった特発性間質性肺炎の内訳は，IPF急性増悪10名であった．治療方法は，当センターの特発性間質性肺炎の急性増悪時治療プロトコールに従い，治療開始時よりメチルプレニゾロン（mPSL）0.5g/日×3日間のミニパルス療法を導入，その後はmPSL250mg/日×3日間，125mg/日×3日間の高用量での減量を行った．さらに維持療法としてPSL0.5mg/kg/日で継続治療を行った．併用療法として，シベレスタットナトリウム投与（4.8mg/kg/日）を最長14日間まで投与を行った（Table 1）．IPF急性増悪の治療経過では，一時改善しても増悪を繰り返すことが多いため，予後評価のためには長い期間を設定するこ

Table 1 Patient populations

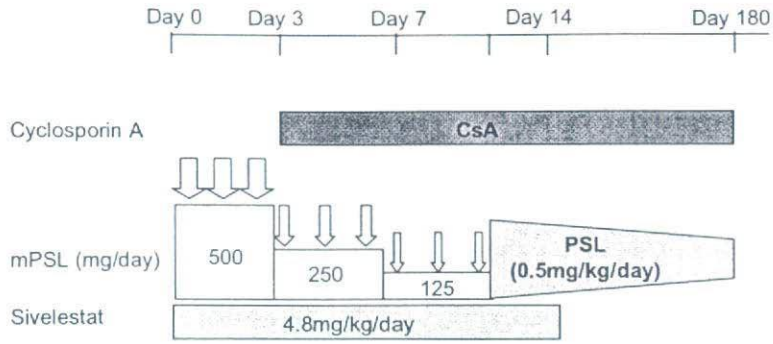

Table 2 Characterization of patient populations

No.	Age	Gender	Diagnosis	Prognosis	Biopsy
1.	76	F	IPF	Alive	No
2.	77	F	IPF	Dead	No
3.	69	M	IPF/UIP	Dead	Yes
4.	78	M	IPF	Alive	No
5.	84	M	IPF	Alive	No
6.	59	M	IPF/UIP	Dead	Yes
7.	70	M	IPF	Dead	No
8.	69	M	IPF	Dead	No
9.	74	M	IPF	Alive	No
10.	79	M	IPF	Dead	No

とが必要と考え，ARDS ネットワークによる臨床研究[7]や過去の臨床研究評価方法を参考に，入院後より 180 日目で生存を評価した．180 日目まで生存した群を生存群，死亡した群を死亡群とした．両群間における，入院時から，0，3，7 日目において，PaO_2/FiO_2 (P/F)，PEEP 値，末梢血中白血球数 (WBC)，血清 CRP 値について経時的検討を行った．また入院時の血清中 KL-6 および SP-D 値の比較検討を行った．統計処理は，unpaired-t test で行い，解析データはすべて平均値±標準誤差 (Mean±SE) で示した．

成　績

生存群は 10 名中 4 名で男性 3 名，女性 1 名（生存率 40%），非生存群は男性 5 名，女性 1 名の合計 6 名であった．対象患者の平均年齢は，72.5±4.8 歳 (Mean±SE) であった．生存群の平均年齢は 77.5±2.6 歳，非生存群で 71.3±2.6 歳と有意差を認めなかった．本研究期間 (2.5 年間) における生存群の平均生存日数は 487±180 (日)，非生存群 22.5±10.4 (日) であった．2 症例は，胸腔鏡下肺生検 (VATS) を施行し，病理組織診断が得られていた (Table 2)．治療開始時の P/F，PEEP 値，WBC 数，CRP 値は各々，P/F (mmHg) は，(生存群 vs 非生存群) ：102.7±33.2，97.5±26.5，PEEP (cmH_2O) 値 (生存群 vs 非生存群) ：8.0±1.3，7.8±1.0，WBC 数 ($cells/mm^3$) (生存群 vs 非生存群) ：10,700±1,286：12,950±3,100，CRP (mg/dl) (生存群 vs 非生存群) ：14.4±6.5，16.0±3.7，と両群間で有意差を認めなかった．上記パラメーターは治療開始後 7 日目での P/F 値は，生存群 222.3±35.5 (mmHg)，非生存群 137.1±29.8 (mmHg) と生存群で有意な改善 ($p<0.05$) を認めた (Fig. 1A)．また生存群で治療開始後 7 日目には PEEP 値の減少 (生存群 vs 非生存群：2.3±1.5，6.0±1.9) ($p<0.05$) が見られた (Fig. 1B)．血液学的データで，WBC 数は治療開始後 7 日目で，生存群で，10,600±1,038 (cells/ml)，非生存群は 14,560±2,480 (cells/ml) で，有意差は認められなかった (Fig. 2A)．CRP 値は治療開始後 7 日目に，生存群 2.5±1.6 (μg/ml)，非生存群 8.4±3.6 (μg/ml) と生存群での有意な改善 ($p<0.05$) が見られた (Fig. 2B)．次に治療開始時，0 日目の血清中 KL-6，SP-D 値を検討した．生存群での治療開始時血清 KL-6 値は，1,008.5±306.6 (ng/ml)，非生存群で，1,942.3±149.4 (ng/ml) と生存群で有意に低値であった ($p<0.05$，Fig. 3)．また，生存群での血清 SP-D 値は，220.1±81.6 (ng/ml)，非生存群では，654.0±122.7 (ng/ml) と，非生存群より有意に低値であった ($p<0.05$，Fig. 4)．

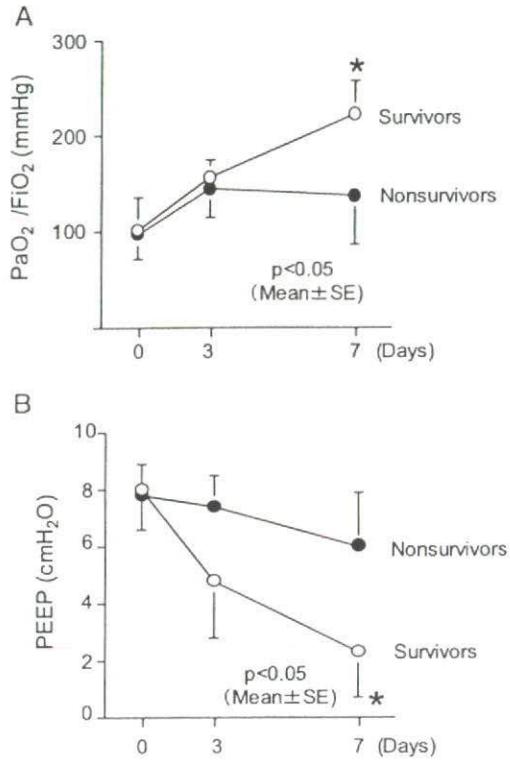

Fig. 1　Time course of PaO_2/FiO_2 (P/F) and PEEP value.
A) P/F improved in survivors on day 7 compared with nonsurvivors. B) PEEP values improved on day 7 in eventual survivors.

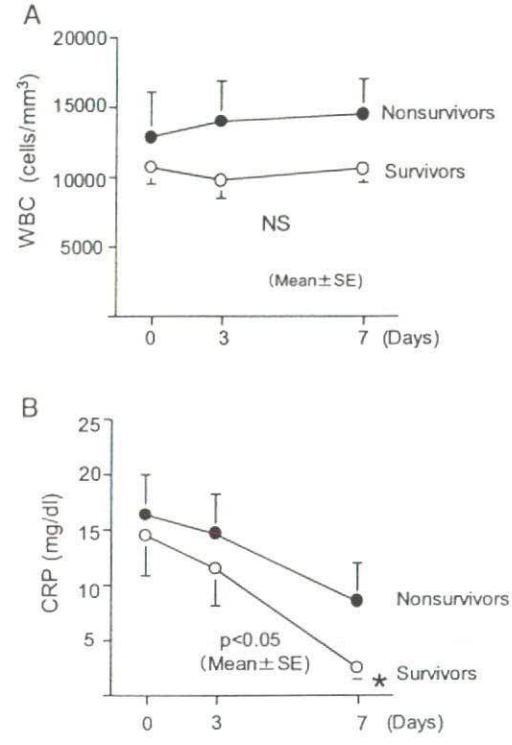

Fig 2　Time course of WBC numbers and CRP value.
A) There was no change between survivors and nonsurvivors. B) CRP values improved in survivors on day 7 compared with nonsurvivors.

考　察

今回我々はIPF急性増悪と診断され，高度の呼吸不全を来たし，人工呼吸器管理となった10名の患者を対象に，180日目の生存率，生存群および非生存群における各種パラメーターの検討，予後因子について検討を行った．IPF急性増悪の治療経過として，一時的に改善しても，増悪を繰り返すことが多い．IPF急性増悪と似た経過をきたす急性呼吸窮迫症候群（ARDS）患者を対象としたARDSネットワークが行っている臨床研究において，治療効果の正確な検討を行うために，生存率の評価日数を最終的に180日としている[7]．本検討でも，このような臨床研究に基づいて生存日数評価を180日目で行った．IPFの急性増悪の予後は極めて予後不良である．過去の報告によれば，IPFの急性増悪例の死亡率は増悪後1カ月以内に65.7%，3カ月以内に94.3%ともされている[5]．また，吉村らはIIP急性増悪35症例の臨床的検討を行い，35症例中28症例（80.1%）が初回増悪時に死亡し，最終的に34症例（97.1%）が19カ月以内に死亡したという報告をしており[8]，特に死亡症例の場合，死亡までの期間は増悪後平均31.5日，増悪後1カ月内死亡率が67.6%と短期間での死亡が際立っていた．さらにIPF進行症例で呼吸不全により人工呼吸器管理を要した患者23症例に関する臨床的検討では，人口呼吸器装着6時間後の平均P/F82±38mmHgであり，60日以内に23症例中22例が死亡という極めて予後不良の報告がされている[9]．本研究においては，全症例の平均P/F 99.6±33.2（mmHg），生存群でも平均P/F 102.7±33.2（mmHg）と高度の呼吸不全を呈しており，極めて重症度の高い患者群で構成されていた．今回の我々の検討では治療開始後180日目の生存率40.0%で，生存群の平均生存日数は487±180（日）で，全例社会復帰し呼吸不全の重症度や過去の臨床的検討と比較し，良好な治療成績と思われた．IPF急性増悪の急性呼吸不全の病態は，ALI/ARDSの病態[10]と非常によく似ており，活性化された好中球から放出される好中球エラスターゼがその病態形成に重要である．好中球エラスターゼは，IPF急性増悪時には血漿および気管支肺胞洗浄液中において増加が報告されている．シベレスタットは，本邦で開発された合成特異的エラスターゼ阻害薬で，ヒト好中球エラスターゼに特異的に拮抗する．IPFの急性増悪時におけるシベレスタットの効果を検討した過去の臨床試験では，第2相試験では良好な成績であったにもかかわらず，最終的に残念ながら第3相試験でシベレスタット使用に

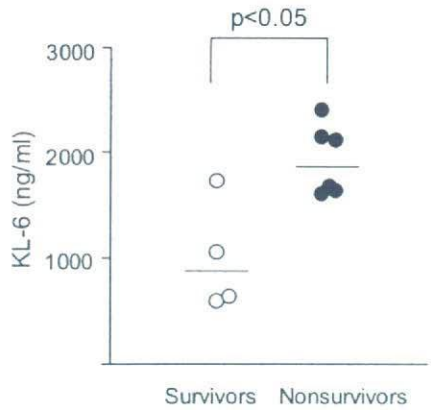

Fig. 3 Serum KL-6 levels on day 0. KL-6 values were significantly lower in eventual survivors compared with nonsurvivors ($p<0.05$).

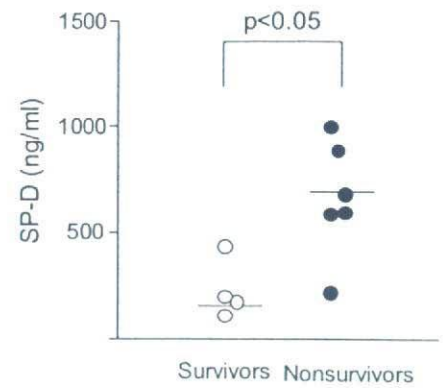

Fig. 4 Serum SP-D levels on day 0. SP-D levels were higher in nonsurvivors compared with eventual survivors.

よる生存率の改善は見られなかった[5]. 今回はシベレスタット未使用群での治療成績については検討を行っていない. しかし, 過去の報告や試験成績や本研究結果を踏まえれば, 症例によっては従来の治療に加えたシベレスタット併用が特発性間質性肺炎の治療においてその有効性が期待できる可能性が示唆された. また特発性間質性肺炎の予後および予後予測因子について過去にいくつかの報告がある. 高橋, Greene らは IPF 患者の血清中 SP-D 濃度が胸部 CT 画像所見の線維化の拡がり, 呼吸機能の低下と相関があり, また血清中の SP-A および SP-D 濃度が IPF 患者の予後と相関するとの報告がある[11][12]. SP-D は肺サーファクタントプロテイン中の一種で, 親水性の糖蛋白質であり, C 型レクチンのコレクチン・サブグループに属し[13][14], IPF 患者の肺機能および P/F の改善や予後との相関度が特に高く, 予後予測因子としての有用性が報告されている[15]. 高橋らは, 血清中 SP-A 及び SP-D 同時高値の症例は急性増悪をきたす可能性があるハイリスク患者となり, 3 年以内に 50% の確率で急性増悪をきたし死亡すると分析し, 予後判定のためのカットオフ値を血清 SP-D 値 220ng/ml に設定した所, 危険群を効率よく抽出することができたと報告している[11]. また血清中 KL-6 濃度も IPF の活動性や予後との高い相関が報告されている[16][17]. KL-6 は, 1985 年に河野らが発見した糖蛋白抗原で, 間質性肺炎の活動性, 線維化の過程の指標とされている[18]. 今回の我々の検討で, 生存群では非生存群と比較し, 治療開始前の血清中 KL-6 値および SP-D 値が低値で, 過去の予後因子を検討した複数の報告結果と合致していた. 血清中 KL-6 および SP-D 測定は簡便かつ非侵襲的で, 安定した結果が得られる検査であり, 特発性間質性肺炎急性増悪症例の予後予測因子として有用であると思われた. 本研究では検討が可能であった症例数が 10 名と少数であるため, 今後はさらに症例数を積み重ね, 検討を加えていく予定である.

なお本内容は, 2006 年アメリカ胸部疾患学会ミニシンポジウム及び 2006 年日本呼吸器学会総会にて発表した.

引用文献

1) Joint Statement of the American Thoracic Society and the European Respiratory Society. Idiopathic pulmonary fibrosis : Diagnosis and treatment. International consensus statement. Am J Respir Crit Care Med 2000 ; 161 : 646—664.
2) Joint Statement of the American Thoracic Society and the European Respiratory Society. American Thoracic Society/European Respiratory Society international Multidisciplinary consensus classification of the idiopathic interstitial pneumonias. Am J Respir Crit Care Med 2002 ; 165 : 277—304.
3) Jeffrey JS, Ware GK, Jennifer KL, et al. Idiopathic pulmonary fibrosis. Challenges and opportunities for the clinician and investigator. Chest 2005 ; 127 : 275—283.
4) Berbhardt GZ, Shozo M, Kazuhito K, et al. Neutrophil elastase and acute lung injury : Prospects for sivelestat and other neutrophl elastase inhibitors as therapeutics. Crit Care Med 2002 ; 30 : S281—S287.
5) 石井芳樹, 北村 諭, 吉良枝郎, 他. 好中エラスターゼ阻害剤 : ONO-5046・Na の特発性間質性肺炎の急性増悪に対する有効性と安全性検討—III 相試験—. 臨床医薬 1998 ; 14 : 421—446.
6) 特発性間質性肺炎の診断・治療ガイドライン. 日本呼吸器学会雑誌 2005 ; 43 : 179—206.
7) The National Heart, Lung and Blood Institute Acute Respiratory Distress Syndrome (ARDS) Clinical Trials Network. Efficacy and safety of coritcosteroids for persistent acute respiratory distress syndrome.

8) 吉村邦彦，中谷龍王，中森祥隆，他．特発性間質性肺炎の急性増悪に関する臨床的検討ならびに考察．日胸疾会誌 1984；22：1012—1020.
9) Jean-Baptiste S, Hervé M, Odile G, et al. Prognosis of patients with advanced idiopathic pulmonary fibrosis requiring mechanical ventilation for acute respiratory failure. Chest 120：213—219.
10) Ware LB, Matthay MA. Medical progress：The Acute Respiratory Distress Syndrome. N Engl J Med 2000；342：1334—1349.
11) Hiroki T, Takuya F, Hiroyuki K, et al. Serum surfactant protein A and D as prognosistic factores in idiopathic pulmonary fibrosis and their relationship to disease extent. Am J Respir Crit Care Med 2000；162：1109—1114.
12) Kelly EG, Talmadge EK Jr, Yoshio K, et al. Serum surfactant protein-A and -D as biomarkers idiopathic pulmonary fibrosis. Eur Respir J 2000；19：439—446.
13) Crouch EC. Collectins and pulmonary host defense. Am J Respire Cell Mol Biol 1998；19：177—120.
14) Crouch EC, Hartshorn K, Ofek I. Collectins and pulmonary innate immunity. Immunol Rev 2000；173：52—65.
15) Yoshio K, Hiroki T, Hirofumi C, et al. Surfactant proteinA and D：Disease Markers. Biochim Biophys Acta 1998；1408：334—345.
16) Jun K, Satoshi K. KL-6：A Serum Marker for Intersitial Pneumonia. Chest 1995；108：311—315.
17) Akihito Y, Nobuyuki K, Hironobu H, et al. Circulating KL-6 predicts the outocome of rapidly progressive idiopathic pulmonary fibrosis. Am J Respir Crit Care Med 1998；158：1680—1684.
18) Hiroshi O, Akihito Y, Keiishi K, et al. Comparative study of KL-6, surfactant protein-A, surfactant protein-D, and monocyte chemoattractant protein-1 as serum markers for interstitial pneumonia. Am J Respir Crit Care Med 2002；165：378—381.

Abstract

The outcome of patients with acute exacerbation of idiopathic interstitial fibrosis (IPF) treated with sivelestat and the prognostic value of serum KL-6 and surfactant protein D

Mari Nakamura, Takashi Ogura, Naoki Miyazawa, Akihiro Tagawa, Satoko Kozawa, Yuji Watanuki and Hiroshi Takahashi
Department of Respiratory Medicine, Kanagawa Cardiovascular and Pulmonary Center

Idiopathic interstitial fibrosis (IPF) is a chronic, usually fatal lung disease of unknown etiology. There are few specific therapies for acute exacerbation of IPF and factors predicting the onset or severity of this syndrome are not clearly understood. A neutrophil elastase inhibitor, sivelestat (ONO-5046) has been commercially available in Japan since 2002. This inhibitor has a potent effect in the treatment of ALI/ARDS. To evaluate the outcome of patients with acute exacerbation of IPF treated with sivelestat and estimate prognostic factors, we investigated 10 patients with acute exacerbation of IPF who were intubated and mechanically ventilated. We analyzed the outcome of patients with acute exacerbation of IPF until day 180 and measured the P/F ratio, PEEP levels, the values of peripheral white blood cell number, and C-reactive protein (CRP) on day 0, 3, 7 after admission. Serum KL-6 and surfactant protein D (SP-D) concentration on day 0 were also analyzed. All patients were treated with sivelestat and methylprednisolone (mPSL) pulse therapy for 3 days from day 0 and maintenance therapy with prednisone (0.5mg/kg/day) were continued. Of the 10 patients, 4 patients had survived (40%) and 6 patients had died (60%) at day 180 from the onset of acute exacerbation of IPF. In survivors, P/F ratio, PEEP levels, and CRP values significantly improved on day 7 ($p<0.05$). Serum KL-6 and SP-D were lower in survivors on day 0 ($p<0.05$). Taken together, serum KL-6 and SP-D may prove valuable as biochemical markers of prognosis in acute exacerbation of IPF. Sivelestat may have potential in the treatment of acute exacerbation of IPF.

Computed Tomography Findings in Pathological Usual Interstitial Pneumonia

Relationship to Survival

Hiromitsu Sumikawa[1], Takeshi Johkoh[1,2], Thomas V. Colby[3], Kazuya Ichikado[4], Moritaka Suga[4], Hiroyuki Taniguchi[5], Yasuhiro Kondoh[5], Takashi Ogura[6], Hiroaki Arakawa[7], Kiminori Fujimoto[8], Atsuo Inoue[1], Naoki Mihara[1], Osamu Honda[1], Noriyuki Tomiyama[1], Hironobu Nakamura[1], and Nestor L. Müller[9]

Departments of [1]Radiology and [2]Medical Physics, Osaka University Graduate School of Medicine, Osaka, Japan; [3]Department of Pathology, Mayo Clinic, Scottsdale, Arizona; [4]Division of Respiratory Medicine, Saiseikai Kumamoto Hospital, Kumamoto, Japan; [5]Department of Respiratory Medicine and Allergy, Tosei General Hospital, Seto, Aichi, Japan; [6]Department of Respiratory Medicine, Kanagawa Cardiovascular and Respiratory Center, Yokohama, Kanagawa, Japan; [7]Department of Radiology, Dokkyo University School of Medicine, Tochigi, Japan; [8]Department of Radiology, Kurume University School of Medicine, Kurume, Japan; and [9]Department of Radiology, University of British Columbia and Vancouver General Hospital, Vancouver, Canada

Rationale: Patients with a clinicopathological diagnosis of idiopathic pulmonary fibrosis (IPF) may have typical findings of usual interstitial pneumonia (UIP) on computed tomography (CT) or nonspecific or atypical findings, including those often seen in nonspecific interstitial pneumonia.

Objectives: The aims of this study were to revisit the high-resolution CT findings of IPF and to clarify the correlation between the CT findings and mortality.

Methods: The study included 98 patients with a histologic diagnosis of UIP and a clinical diagnosis of IPF. Two observers evaluated the CT findings independently and classified each case into one of the following three categories: (*1*) definite UIP, (*2*) consistent with UIP, or (*3*) suggestive of alternative diagnosis. The correlation between the CT categories and mortality was evaluated using the Kaplan-Meier method and the log-rank test, as well as Cox proportional hazards regression models.

Measurements and Main Results: Thirty-three of the 98 CT scans were classified as definite UIP, 36 as consistent with UIP, 29 as suggestive of an alternative diagnosis. The mean survival was 45.7, 57.9, and 76.9 months, respectively. There was no significant difference in survival among the three categories (all $P > 0.05$). Traction bronchiectasis and fibrosis scores were significant predictors of outcome (hazard ratios: 1.30 and 1.10, respectively; 95% confidence intervals: 1.18–14.2 and 1.03–1.19, respectively).

Conclusions: In patients with IPF and UIP pattern on the biopsy, the pattern of abnormality on thin-section CT, whether characteristic of UIP or suggestive of alternative diagnosis, does not influence prognosis. Prognosis is influenced by traction bronchiectasis and fibrosis scores.

Keywords: interstitial pneumonia; idiopathic pulmonary fibrosis; high-resolution computed tomography; lung

AT A GLANCE COMMENTARY

Scientific Knowledge on the Subject

Few previous reports have described the CT findings of UIP diagnosed according to the current histopathological criteria and the frequency of patients with IPF who have atypical CT findings. In addition, it is still unclear which CT findings influence the prognosis.

What This Study Adds to the Field

In patients with IPF and UIP pattern on the biopsy, the pattern of abnormality on thin-section CT, whether characteristic of UIP or suggestive of alternative diagnosis, does not influence prognosis. Prognosis is influenced by traction bronchiectasis and fibrosis scores.

According to the American Thoracic Society (ATS) and European Respiratory Society (ERS) 2002 Working Group Consensus Classification of Idiopathic Interstitial Pneumonias (IIPs), the primary role of thin-section computed tomography (CT) is to separate patients with characteristic findings of idiopathic pulmonary fibrosis (IPF)/usual interstitial pneumonia (UIP) from those with other IIPs (1). Previous reports have stated that the characteristic CT findings of UIP include the following: honeycombing, reticular opacities, ground-glass attenuation, and both basal and peripheral predominance, which is often associated with traction bronchiectasis and architectural distortion (2–4).

Thin-section CT is useful for differentiating IPF/UIP from other IIPs (5–7). However, even experienced radiologists sometimes confuse IPF/UIP with other IIPs, especially nonspecific interstitial pneumonia (NSIP) (5, 6, 8, 9). This implies that the CT findings of patients with a histologic diagnosis of UIP and a clinical diagnosis of IPF include not only patients with characteristic findings of UIP on CT but also patients with an NISP pattern or nonspecific or atypical CT findings. Few previous reports have described the CT findings of UIP diagnosed according to the current histopathological criteria and the frequency of patients with IPF who have atypical CT findings. In addition, it is still unclear which CT findings influence the prognosis. This study had two aims: to revisit the thin-section CT findings of IPF and to clarify the correlation between CT findings and mortality.

METHODS

Patients and Diagnoses

The ethical review boards of the three institutions that contributed cases to the present study did not require the patients' approval or informed consent for the retrospective review of their records and images.

One hundred and fifty-four patients who underwent surgical biopsies at three institutions and who met the clinical and histologic criteria for diagnosis recommended by the ATS/ERS consensus classification of the IIPs were identified (1). All 154 cases were originally diagnosed histologically as diagnostic of UIP by a lung pathologist at each of the

(*Received in original form November 23, 2006; accepted in final form October 29, 2007*)

Correspondence and requests for reprints should be addressed to Hiromitsu Sumikawa, M.D., Department of Radiology, Osaka University Graduate School of Medical, 2-2 Yamadaoka, Suita, Osaka, 565-0825, Japan. E-mail: h-sumikawa@radiol.med.osaka-u.ac.jp

Am J Respir Crit Care Med Vol 177. pp 433–439, 2008
Originally Published in Press as DOI: 10.1164/rccm.200611-1696OC on November 1, 2007
Internet address: www.atsjournals.org

contributing institutions. All biopsy specimens were also reviewed by a second lung pathologist with 32 years of experience and classified into the following four categories by the certainty of the diagnosis of UIP: (*1*) confident UIP, (*2*) probable UIP, (*3*) probably not UIP, and (*4*) confident not UIP. A confident diagnosis of UIP was made if all the ATS/ERS criteria were fulfilled: patchy involvement with clear evidence of chronic scarring/honeycombing and the presence of fibroblast foci in the absence of features against the diagnosis of UIP, such as granulomas and so forth. A confident diagnosis of "not UIP" was made if there were clear features of an alternative diagnosis, or if none of the ATS/ERS criteria for UIP were present. Diagnoses of "probable UIP" and "probably not UIP" were more subjective; most commonly the former represented cases of extensive honeycombing without good evidence of patchy involvement in the sample reviewed, and the latter were cases in which the histology was more suggestive of an alternative diagnosis. On the basis of this review, 112 cases (73%) were diagnosed as definite UIP, 19 cases (12%) as probable UIP, 16 cases (10%) as probably not UIP, and 7 cases (5%) as confidently not UIP. Only the 112 cases interpreted by the second lung pathologist as definitely being UIP were considered acceptable for the study. Of these, 14 had to be excluded because their CT scans were not available or they had the other diseases in the lungs. The study therefore included 98 patients who had a confident histologic diagnosis of UIP made by two independent lung pathologists and who had a clinical diagnosis of IPF. The study sample consisted of 71 men and 27 women, with a mean age of 63 years (range, 36–75 yr). Survival analysis, survival status, and follow-up periods were assessed by review of the medical records. The mean and median follow-up periods of all cases were 79 and 63 months, respectively. Forty-six patients died and 10 were lost to follow-up.

Thin-Section CT Images and Review

Thin-section CT scans of all patients were obtained at end inspiration and in the supine position using a variety of scanners. The mean period from CT scan to surgical biopsy was 35 days (range, 1–411 d). The protocols consisted of 1–2-mm collimation sections reconstructed with a high-spatial-frequency algorithm at 1- or 2-cm intervals. The images were photographed at window settings appropriate for viewing the lung parenchyma (window level from –600 to –700 Hounsfield units [HU]; window width from 1,200 to 1,500 HU). The images were reviewed in random order by four radiologists. All observers were chest radiologists with 20, 18, 15, and 7 years of experience, respectively. The four radiologists were divided into two groups of two radiologists each. In each group, the images were assessed independently, and the findings were agreed upon by consensus between the two radiologists. All radiologists were informed about pathological and clinical UIP diagnosis.

The radiologist evaluated the presence, extent, and distribution of CT findings, which included the presence of ground-glass attenuation, airspace consolidation, nodules, interlobular septal thickening, thickening of bronchovascular bundles, intralobular reticular opacities, irregular interlobular septal thickening, nonseptal linear or platelike opacities, presence of honeycombing, cysts, emphysema, architectural distortion, traction bronchiectasis, and fibrosis score. The definitions of each CT finding are shown in Table 1.

The observers evaluated the extent of all radiologic abnormalities, excluding emphysema, that were present in both lungs to determine the percentage of lung parenchyma occupied by the disease. The lungs were divided into six zones (upper, middle, and lower on both sides); each zone was evaluated separately. The upper lung zone was defined as the area of the lung above the level of the tracheal carina, the lower lung zone was defined as the area of the lung below the level of the inferior pulmonary vein, and the middle lung zone was defined as the area of the lung between the upper and lower zones. When abnormal findings were present, the extent of lung involvement was evaluated visually and independently for each of the six lung zones. The score was based on the percentage of the lung parenchyma that showed evidence of the abnormality and was estimated to the nearest 5% of parenchymal involvement. The overall percentage of lung involvement was calculated by averaging the six lung zones.

The extent of traction bronchiectasis was quantified by assessing the generations of the most proximal bronchial branches that were involved. Traction bronchiectasis was scored as follows: 0, none; 1, bronchial dilatation involving bronchi distal to the fifth generation; 2, bronchial dilatation involving fourth-generation bronchi; 3, bronchial dilatation involving bronchi proximal to the third-generation bronchi. These scores were assessed in each of the six lung zones and the overall score of traction bronchiectasis was obtained by adding the scores of the six lung zones. For each lung zone, architectural distortion was scored as 0 (absent) or 1 (present), and all of the scores were summed. To evaluate interstitial fibrosis, in each zone a fibrosis score was assigned: 0, none; 1, ground-glass attenuation without reticulation; 2, ground-glass and fine reticular opacity; 3, reticular opacity and microcysts less than 3 mm; or 4, coarse reticular opacity and large cysts more than 3 mm (6). These scores were assessed for each of the six lung zones and then summed. Furthermore, the extent of disease close to the hilum was scored as follows: 1, abnormal parenchyma distal to the fifth-generation bronchus; 2, abnormal parenchyma distal to the fourth-generation bronchus; 3, abnormal parenchyma proximal to the third-generation bronchus. The observers also provided an overall evaluation of their impression of the CT findings as to whether they were homogeneous or heterogeneous. After assessing the presence and extent of the findings, the observers evaluated their predominant distribution. The distribution was classified as being predominantly upper, lower, peripheral, dependent, or peribronchovascular. Asymmetrical predominance was considered to be present if the extent of findings or the degree of fibrosis was predominant on one side. The overall extent of various abnormal findings was obtained by averaging the evaluation by the two independent observers. Disagreements with respect to architectural distortion, traction bronchiectasis, fibrosis score, extent of disease toward the hilum, impression of diseases, and predominant distribution were resolved by consensus.

After review of the findings, the CT scans in each case were classified by consensus between the four observers into those that were

TABLE 1. DEFINITION OF EACH COMPUTED TOMOGRAPHY FINDING

CT Finding	Definition
Ground-glass attenuation	Hazy increased attenuation of the lung that did not obscure the underlying vessels
Airspace consolidation	Homogeneous increase in pulmonary parenchymal attenuation that obscured the underlying vessels
Nodules	Small nodular opacities with a clear border
Interlobular septal thickening	Abnormal widening of the interlobular septa
Thickening of bronchovascular bundles	Increase in bronchial wall thickness and in the diameter of pulmonary artery branches caused by thickened peribronchovascular interstitium
Regular intralobular reticular opacities	Regular interlacing linear shadows separated by a few millimeters and typically superimposed on ground-glass opacities and resulting in "crazy-paving" pattern
Irregular intralobular reticular opacity	Irregular and randomized linear shadows separated by a few millimeters were seen
Nonseptal linear or platelike opacity	Elongated line of soft tissue attenuation that was distinct from interlobular septa and bronchovascular bundles
Honeycombing	Clustered cystic airspaces from several millimeters to 1 centimeter in size with well-defined and thick walls were seen in the subpleural regions
Emphysema	Focal region of low attenuation without visible walls
Cysts	Round airspaces with a well-defined wall
Architectural distortion	Abnormal displacement of bronchi, pulmonary vessels, interlobar fissures, or interlobular septa
Traction bronchiectasis	Irregular bronchial dilatation within or around areas with parenchymal abnormality

radiologically consistent with UIP or those that were suggestive of an alternative diagnosis based on the results of previous studies that reported the thin-section CT appearance of UIP (1–4). The detailed classification was as follows: (*1*) definite UIP, (*2*) consistent with UIP, or (*3*) suggestive of alternative diagnosis. The CT scan was classified as showing a definite UIP pattern when it demonstrated honeycombing in a predominantly peripheral and basal distribution. The CT was classified as consistent with UIP when it demonstrated a reticular pattern in a predominantly peripheral and basal distribution but only minimal or no honeycombing. The CT was classified as suggestive of alternative diagnosis when alternatives to UIP, such as NSIP, were more appropriate. The relationship between survival duration and these three CT categories as subtypes was evaluated.

Statistical Analysis

All statistical analyses were performed using SPSS statistical software (version 12.0J, 2003; SPSS, Inc., Chicago, IL). The interobserver variation of the extent of the various abnormalities (architectural distortion, traction bronchiectasis, disease distribution toward the hilum, and fibrosis score) was evaluated using Spearman's rank correlation coefficient. The interobserver variation of the existence of predominant distribution and the overall impression of the findings was analyzed using the κ statistic. Interobserver agreement was classified as follows: poor (κ = 0–0.20), fair (κ = 0.21–0.40), moderate (κ = 0.41–0.60), good (κ = 0.61–0.80), and excellent (κ = 0.81–1.00).

Comparison between definite UIP and the other two CT categories of abnormality was made using univariate analysis. The extent of the individual CT patterns, traction bronchiectasis, disease distribution toward the hilum, and fibrosis score were assessed using the Mann-Whitney U test. The presence of architectural distortion, predominant distribution, and the overall impression was analyzed using Fisher exact test. Univariate and multivariate Cox proportional hazards regression models were used to identify independent CT predictors of outcome. On multivariate analysis, the variables were selected using a stepwise procedure including each one of the following CT findings: presence of ground-glass attenuation; airspace consolidation; nodules; interlobular septal thickening; thickening of bronchovascular bundles; intralobular reticular opacities; irregular interlobular septal thickening; nonseptal linear or platelike opacities; presence of honeycombing, cysts, emphysema, architectural distortion, or traction bronchiectasis; fibrosis score; the extent of disease close to the hilum; and upper, lower, peripheral, dependent, peribronchovascular, and asymmetric predominant distribution. Findings were retained if they contributed to the power of the regression equation ($P < 0.10$).

Patient survival between the three CT categories (1, definite UIP; 2, consistent with UIP; and 3, suggestive of alternative diagnosis) was determined using the log-rank test and displayed using Kaplan-Meier curves. A P value of less than 0.05 was considered to indicate statistical significance.

RESULTS

Observer Agreement and Diagnoses

Interobserver agreement (Table 2) was poor to good with respect to the extent of the various abnormalities (Spearman rank correlation coefficient, r = 0.13–0.79; $P < 0.001$–0.19), with poor to moderate agreements for the presence of architectural distortion and the predominant distribution (κ = 0–0.56). Interobserver agreement was poor for the presence of nodules (r = 0.19), thickening of bronchovascular bundles (r = 0.15), nonseptal linear opacity (r = 0.13), and dependent distribution (κ = 0). The interobserver agreement of CT diagnosis into consistent with UIP (definite or probable) or suggestive of alternate diagnosis (suggestive of NSIP or indeterminate) was moderate (κ = 0.60).

TABLE 2. THE EXTENT OF COMPUTED TOMOGRAPHY FINDINGS, INTEROBSERVER CORRELATION, AND PREDICTORS OF OUTCOME ON UNIVARATE ANALYSIS WITH COX PROPORTIONAL HAZARDS REGRESSION MODELS

		Interobserver Correlation		Predictor of Outcome	
CT Findings	Extent	r or κ Value	P Value	Hazard Ratio	95% CI
All abnormalities	35.6 ± 13.5*	0.76†	<0.001‡	1.05	1.02–1.07
Ground-glass attenuation	23.4 ± 11.3*	0.68†	<0.001‡	1.01	0.99–1.04
Airspace consolidation	4.4 ± 5.6*	0.69†	<0.001‡	1.10	1.03–1.17
Nodules	2.8 ± 1.6*	0.19†	0.07	1.06	0.88–1.29
Interlobular septal thickening	3.6 ± 5.1*	0.38†	<0.001‡	1.01	0.96–1.06
Thickening of BVB	0.4 ± 1.6*	0.15†	0.14	0.95	0.76–1.12
Regular intralobular reticular opacity	0.9 ± 3.2*	0.42†	<0.001‡	0.87	0.68–1.13
Irregular intralobular reticular opacity	11.8 ± 6.8*	0.66†	<0.001‡	1.04	1.00–1.09
Nonseptal linear opacity	0.8 ± 1.4*	0.13†	0.19	0.89	0.61–1.29
Honeycombing	4.2 ± 5.8*	0.80†	<0.001‡	1.05	1.01–1.09
Cysts	3.9 ± 3.2*	0.52†	<0.001‡	1.01	0.93–1.10
Emphysema	2.8 ± 7.1*	0.68†	<0.001‡	0.88	0.77–1.01
Architectural distortion	4.9 ± 1.3§	0.35†	<0.001‡	1.72	1.26–2.34
Traction bronchiectasis	5.1 ± 3.5§	0.75†	<0.001‡	1.31	1.20–1.44
Fibrosis score	16.7 ± 4.5§	0.79†	<0.001‡	1.12	1.05–1.2
Extent of disease toward hilum	1.6 ± 0.8§	0.56†	<0.001‡	1.34	0.90–1.99
Homogeneous impression	83‖	0.53¶	<0.001‡	4.30	1.03–17.95
Upper predominance	1‖	NA	NA	0.05	0–684
Lower predominance	77‖	0.5¶	<0.001‡	0.60	0.29–1.24
Peripheral predominance	76‖	0.5¶	<0.001‡	0.78	0.36–1.71
Dependent predominance	3‖	NA	NA	0.63	0.09–4.65
Peribronchovascular predominance	4‖	0.47¶	<0.001‡	0.49	0.07–3.57
Symmetry	74‖	0.44¶	<0.001‡	1.55	0.81–3.00

Definition of abbreviations: BVB = bronchovascular bundles; CI = confidence interval; NA = no answer (it cannot be calculated).

* Mean percentage of lung parenchyma ± SD.

† r Value with Spearman's rank correlation.

‡ There was a statistically significant difference ($P < 0.05$).

§ Mean scores ± SD. Scores are defined in METHODS.

‖ Number of cases with a feature.

¶ κ Value with κ analysis.

The observers classified 33 cases (34%) as having definite UIP (Figure 1), 36 as consistent with UIP (Figure 2), 21 (21%) as having CT findings suggestive of NSIP (Figure 3), and 8 cases (8%) as having unclassified findings (Figure 4).

Predominant Findings

The total CT findings of all cases are shown in Table 2. Ground-glass attenuation (23.4%) and intralobular irregular reticular opacities (11.8%) were the most common findings, whereas thickening of bronchovascular bundles (0.4%), intralobular regular reticular opacities (0.9%), and nonseptal linear opacities (0.8%) were the least common findings. Lower zone predominance (n = 77) and peripheral predominance (n = 76) were common. Seventy-four patients had symmetric bilateral distribution of findings and 24 had asymmetric distribution.

The CT findings of each CT category are shown in Table 3. As compared with patients with CT findings classified as definite UIP, patients with findings consistent with UIP were more likely to have airspace consolidation (5.2%), interlobular septa (3.4%), regular intralobular reticular opacity (0.4%), and emphysema (3.0%), and less likely to have honeycombing (1.8%) and cysts (2.9%) ($P < 0.05$). Patients with CT findings suggestive of alternative diagnosis were more likely to have ground-glass attenuation (28.4%), airspace consolidation (6.2%), interlobular septal thickening (5.9%), regular reticular opacity (2.6%), and peribronchovascular distribution (n = 4), and less likely to have honeycombing (1.7%) ($P < 0.05$).

The results of Cox regression analysis for the relationship between the CT findings and prognosis are shown in Tables 2 and 4. On univariate analysis, all abnormalities, including airspace consolidation, honeycombing, architectural distortion, traction bronchiectasis, fibrosis score, and heterogeneous overall impression, were significant predictors (hazard ratios: 1.05, 1.10, 1.05, 1.72, 1.31, 1.12, and 4.30, respectively). On multivariate analysis, only traction bronchiectasis and fibrosis score were significant predictors of mortality (hazard ratios: 1.30 and 1.10, respectively).

CT Pattern of Abnormality and Mortality

The Kaplan-Meier survival curves and their relation to the pattern of abnormality on CT are shown in Figure 4. The mean survivals of patients with CT findings interpreted as definite UIP, consistent with UIP, suggestive of alternative diagnosis categories were 45.7, 57.9, and 76.9 months, respectively, and the median survivals were 34.8, 43.4, and 112 months, respectively. The prognosis of definite UIP was not significantly different from that of the other two categories (log-rank test: $P = 0.26$ and 0.09, respectively).

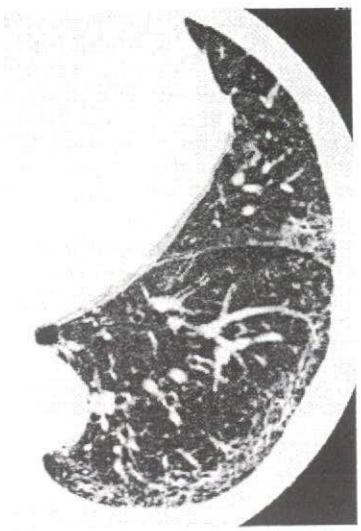

Figure 2. A pattern consistent with a usual interstitial pneumonia in a 62-year-old man. Transverse computed tomography (CT) images obtained with 2-mm section thickness. Thin-section CT image through the left lower lobe demonstrates irregular intralobular reticular opacity, ground-glass opacity, and traction bronchiectasis in a predominantly peripheral distribution.

DISCUSSION

All 98 patients in this study had a pathological diagnosis of definite UIP. The most common findings in the cases classified as having definite UIP radiologically were honeycombing, irregular intralobular reticular opacities, and ground-glass opacities. This result agrees with previous reports of CT findings of UIP (2, 4, 9, 10). However, in the present study, an asymmetric distribution was seen more often than expected, in 24 of 98 patients. An asymmetric distribution may reflect a temporal heterogeneity between the right and left lungs and may be a characteristic finding of UIP. However, further assessment, including cases with NSIP, is necessary to further clarify this issue.

Cases in the probable UIP category radiologically had irregular reticular opacities and ground-glass opacities in the lower and peripheral lung. These findings are compatible with UIP but the lack of peripheral and basal honeycombing on CT precluded a confident diagnosis. The findings on CT may be

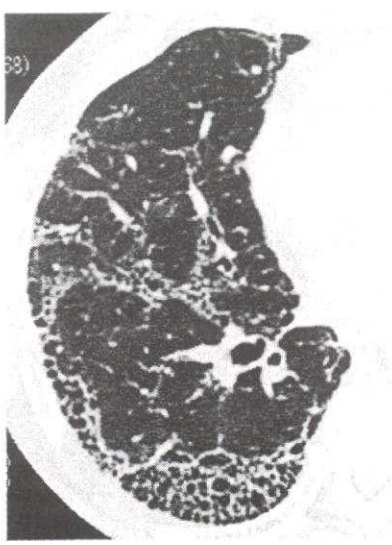

Figure 1. Definite usual interstitial pneumonia pattern in a 57-year-old man. Transverse computed tomography (CT) images obtained with 2-mm section thickness. Thin-section CT image through the right lower lobe demonstrates honeycombing in a predominantly peripheral distribution.

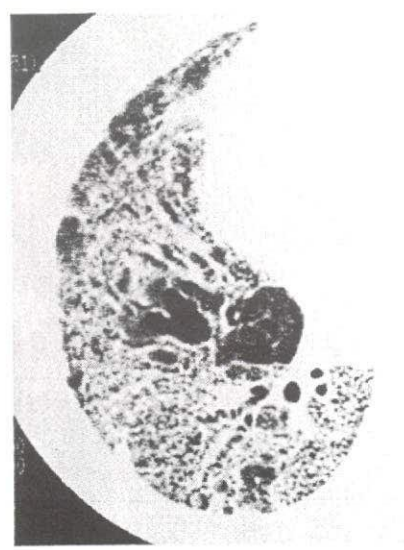

Figure 3. Pattern suggestive of alternative diagnosis in a 68-year-old woman. Thin-section (2-mm collimation) computed tomography image through the right lower lobe demonstrates ground-glass opacity, airspace consolidation, irregular intralobular reticular opacity, and traction bronchiectasis.

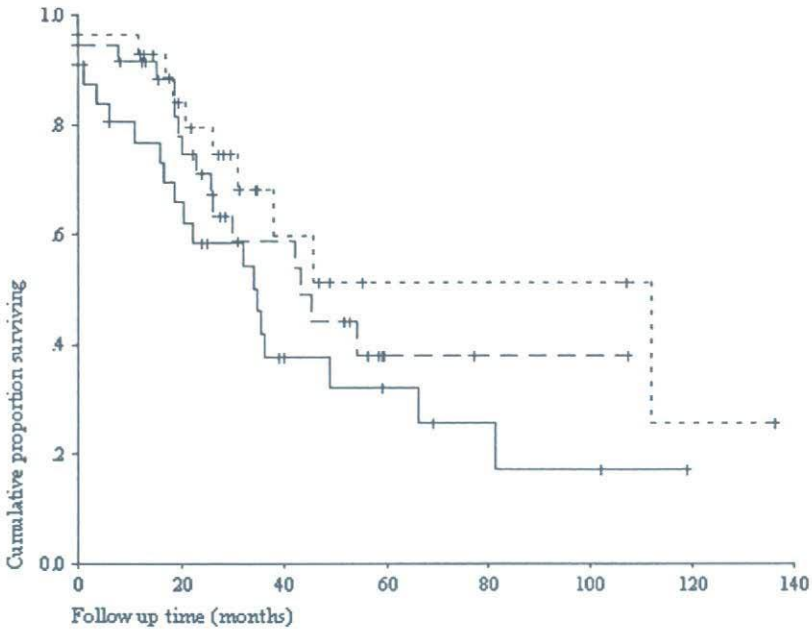

Figure 4. Kaplan-Meier survival curves for cases with definite usual interstitial pneumonia (UIP) (n = 33, *solid line*), findings consistent with UIP (n = 36, *dashed line*), and findings suggestive of alternative diagnosis (n = 29, *dotted line*).

indicative of early UIP. However, there was no difference in the mortality of definite UIP and consistent with UIP cases. Some cases with these findings had areas of airspace consolidation, which pathologically sometimes reflect airless fibrotic tissue or honeycombing filled with mucinous secretions (4, 11); and dependent atelectasis would cover the other findings. For such reasons, CT may underestimate the extent of honeycombing and thus the severity of fibrosis.

As previously shown, there is overlap between the high-resolution CT (HRCT) findings of UIP and those of NSIP (6, 12–14). Therefore, not surprisingly, several of our patients had CT findings interpreted as suggestive of alternative diagnosis, and 21 of 29 cases with an alternative diagnosis had CT findings similar to NSIP. It must be pointed out that a confident diagnosis of NSIP requires surgical biopsy. It should also be noted that regions showing pathological NSIP are described in

TABLE 3. COMPARISON OF COMPUTED TOMOGRAPHY FINDINGS BETWEEN DEFINITE USUAL INTERSTITIAL PNEUMONIA AND OTHER COMPUTED TOMOGRAPHY CATEGORIES

	Definite UIP (*n* = 33)	Consistent with UIP (*n* = 36)		Suggestive of Alternative Diagnosis (*n* = 21)	
CT Findings	Extent	Extent	*P* Value	Extent	*P* Value
All abnormalities	34.8 ± 11.3*	32.5 ± 15.0*	0.21	40.2 ± 12.8*	0.12
Ground-glass attenuation	18.9 ± 9.9*	23.5 ± 11.9*	0.14	28.4 ± 10.1*	0.001†
Airspace consolidation	1.9 ± 2.3*	5.2 ± 7.4*	0.04†	6.2 ± 4.9*	<0.001†
Nodules	2.9 ± 1.8*	2.5 ± 1.0*	0.80	3.0 ± 2.0*	0.75
Interlobular septal thickening	1.8 ± 2.0*	3.4 ± 3.6*	0.02†	5.9 ± 7.8*	<0.001†
Thickening of BVB	0.1 ± 0.3*	0.4 ± 1.3*	0.50	0.7 ± 2.5*	0.105
Regular intralobular reticular opacity	0.0 ± 0.0*	0.4 ± 1.4*	0.05	2.6 ± 5.3*	<0.001†
Irregular intralobular reticular opacity	11.4 ± 7.0*	12.5 ± 6.3*	0.31	11.2 ± 7.2*	0.94
Nonseptal linear opacity	0.5 ± 0.7*	0.8 ± 0.9*	0.13	1.1 ± 2.2*	0.23
Honeycombing	9.1 ± 6.9*	1.8 ± 2.4*	<0.001†	1.7 ± 3.7*	<0.001†
Cysts	6.0 ± 3.9*	2.9 ± 1.7*	<0.001†	2.8 ± 2.6*	0.001†
Emphysema	3.0 ± 4.1*	3.5 ± 10.2*	0.03†	1.6 ± 4.7*	0.02†
Architectural distortion	5.1 ± 1.2‡	4.5 ± 1.5‡	0.13	5.2 ± 1.2‡	0.62
Traction bronchiectasis	4.9 ± 3.6‡	4.7 ± 3.4‡	0.92	5.8 ± 3.4‡	0.15
Fibrosis score	20.2 ± 3.6‡	15.3 ± 3.9‡	<0.001†	14.6 ± 3.7‡	<0.001†
Extent of disease toward hilum	1.3 ± 0.5‡	1.3 ± 0.6‡	0.51	2.2 ± 0.8‡	<0.001†
Heterogeneous impression	33§	35§	NS	15§	<0.001†
Upper predominance	0§	0§	NS	1§	0.47
Lower predominance	28§	30§	NS	19§	0.14
Peripheral predominance	33§	32§	0.12	11§	<0.001†
Dependent predominance	1§	1§	NS	1§	1
Peribronchovascular predominance	0§	0§	NS	4§	0.04†
Symmetry	22§	30§	0.16	22§	0.58

Definition of abbreviations: BVB = bronchovascular bundles; NS = not significant; UIP = usual interstitial pneumonia.

* Mean percentage of lung parenchyma ± SD.

† There was a statistically significant difference from definite UIP ($P < 0.05$).

‡ Mean scores ± SD. Scores are defined in METHODS.

§ Number of cases with a feature.

TABLE 4. THE PREDICTOR OF OUTCOME IN MULTIVARIATE ANALYSIS WITH COX PROPORTIONAL HAZARDS REGRESSION MODELS

CT Findings	Hazard Ratio	95% Confidence Interval
Traction bronchiectasis	1.30	1.18–1.43
Fibrosis score	1.10	1.03–1.19

patients who have biopsy-confirmed UIP in surgical lung biopsies (15, 16). Cases with histologic regions showing both UIP and NSIP have a prognosis similar to patients with UIP and are therefore considered to have "histologic discordant UIP." Although all of the obtained biopsy specimens in the current study had characteristic histologic features of UIP, it is possible that other areas of the remaining lungs had findings of NSIP.

Some cases having findings suggestive of alternative diagnosis had various CT findings, but in each case the findings on CT did not allow for classification into any of the categories of IIPs based on the ATS/ERS consensus (1). Hartman and colleagues reported that the appearance of NSIP on CT was variable and included the findings of UIP and those of other chronic infiltrative lung diseases (14). They suggested that the presence of a histologic spectrum of NSIP or sampling error of the biopsy specimens could explain the variability of CT findings (14). The findings of UIP would vary on CT, likely due to the variability in the histology of NSIP.

In the current study, 29 of 98 patients (30%) with UIP had HRCT findings that were interpreted as more consistent with an alternate diagnosis. Thus, almost one-third of cases with histologic UIP had CT features suggestive of other diseases, especially NSIP. This result is compatible with previous reports (5, 6, 8, 9). In histologically confirmed UIP cases, there were some cases in which the CT findings were identical to those of NSIP. The current study only included cases that had surgical biopsy–proven diagnosis. In clinical practice, patients with characteristic CT findings of IPF/UIP in accordance with ATS/ERS consensus statement usually do not require biopsy (1). Therefore, our study is biased toward patients with atypical CT findings of IPF. This selection bias presumably accounts for the relatively high extent of ground-glass opacity (mean extent, 23.4%) and the presence of consolidation (mean extent, 4.4%) in our patients with UIP. The relatively high extent of ground-glass opacity also accounted for the high mean overall extent of abnormality (36%). The fact that the extent of ground-glass opacity was greater than reticulation (11.8%) is quite atypical for UIP, and reflects a skewed population, because patients with characteristic features of UIP seldom undergo surgical biopsy.

The prognosis of IPF in our study was poor, and there was no significant difference in prognosis between cases with typical CT findings of UIP and those with atypical findings. Previous studies have shown that the prognosis of IPF/UIP is poor and that the prognosis of NSIP is better than that of IPF/UIP (15, 17–19). In histologically diagnosed UIP cases, Flaherty and colleagues reported that the prognosis of cases that were diagnosed as UIP based on both CT and histologic findings was worse than in cases with a histologic diagnosis of UIP but without CT features of UIP (20). However, in their previous report, the difference in prognosis was small, and the prognosis of cases with a histologic diagnosis of NSIP was much better (20). Our study included only the cases with definite diagnosis of UIP in histology, and the shorter survival time in the cases with atypical CT pattern could be overestimated. The relatively small number of cases may also have been a factor. There may also have been some preselection bias. Cases were selected solely on the basis of definite UIP histologically confirmed by at least two observers, which might have led to a smaller number of cases than would have resulted if some of the histologically "probable" UIP cases were included. However, the causes for the discrepancy between our study and Flaherty and colleagues' are not clear. The results of our study suggest that the prognosis of cases with histologic diagnosis of UIP is poor even if they have atypical CT findings.

Various CT findings were found to influence outcome in our study. On univariate analysis, total amount of all abnormalities, airspace consolidation, honeycombing, architectural distortion, traction bronchiectasis, fibrosis score, and the overall impression of the CT findings influenced the outcome significantly, whereas, on multivariate analysis, only traction bronchiectasis and fibrosis score influenced outcome significantly. These findings are mainly associated with the degree and extent of lung fibrosis, and the results of the present study are similar to those of a previous report (21). Correlations between observers for traction bronchiectasis and fibrosis score were good (0.75 and 0.79, respectively). In the present study, the CT category was determined not only by specific CT findings but also by their distribution. In particular, the determination of concordant UIP was strongly based on the distribution of the findings. However, the distribution of the findings did not affect the mortality on both univariate and multivariate analyses. Therefore, the CT category is not helpful in predicting the outcome.

Our study has several limitations. First, the study was retrospective. The treatments given patients were not identical and this may have influenced the evaluation of prognosis. Second, the study included only patients who had surgical biopsy, and thus had a selection bias with a higher proportion of patients with atypical CT findings of IPF/UIP than would be seen in daily clinical practice. In addition, the observers knew that all patients had clinical and histological UIP. This fact would influence the interpretation and diagnosis in HRCT. Thirty percent of all cases were diagnosed as not having UIP; however, the number of cases would increase in blind reading. Another limitation of this study is that it was limited to the correlation of the initial CT findings with survival data. It did not include correlations of survival or CT data with functional parameters. The study also included relatively few patients. Although there was no significant difference in survival between patients with CT findings consistent with UIP and those with findings more suggestive of NSIP, the mean survival of patients with CT findings interpreted as definite UIP was 45.7 months, compared with 57.9 months for patients with CT scans interpreted as being probable UIP, and 76.9 months for patients with CT scans interpreted as suggestive of alternative diagnosis. These results suggest a trend toward greater survival of patients with CT findings more suggestive of alternative diagnosis. Furthermore, there was a strong trend ($P = 0.07$) that the extent of disease in patients with CT findings more suggestive of alternative diagnosis was more extensive than that in those with CT findings typical of UIP. The lack of statistical difference between the various groups may be due to the relatively small number of patients in the study. Therefore, the study cannot be used to refute the findings by Flaherty and colleagues that patients with IPF who have atypical CT findings have a better prognosis than patients with characteristic CT findings of UIP. In addition, only one pathologist decided on the final pathological diagnosis in this study. All 154 cases were originally diagnosed histologically as diagnostic of UIP by a lung pathologist at each of the participating institutions, then all biopsy specimens were reviewed by a second lung pathologist. Therefore, more than two pathologists diagnosed the cases as UIP; however, they did not diagnose independently, and the interobserver variation could not be evaluated. The other limitation is that the histologic diagnoses based on surgical biopsies may

have had a sampling error. The histologic diagnosis of multiple specimens from one patient may sometimes differ (15). Finally, some CT variables were collated with each other, such as honeycombing and fibrosis score. Therefore, honeycombing might not be a predictor of poor outcome in multivariate analysis, although honeycombing was a predictor in univariate analysis.

In conclusion, cases with pathologically proven IPF/UIP had greater variability in their CT findings than expected; however, there was no significant difference in mortality between the various CT categories. Traction bronchiectasis and fibrosis score were predictors of poor outcome.

Conflict of Interest Statement: None of the authors has a financial relationship with a commercial entity that has an interest in the subject of this manuscript.

References

1. American Thoracic Society; European Respiratory Society. American Thoracic Society/European Respiratory Society international multidisciplinary consensus classification of the idiopathic interstitial pneumonias. *Am J Respir Crit Care Med* 2002;165:277–304.
2. Akira M, Sakatani M, Ueda E. Idiopathic pulmonary fibrosis: progression of honeycombing at thin-section CT. *Radiology* 1993;189:687–691.
3. Muller NL, Miller RR, Webb WR, Evans KG, Ostrow DN. Fibrosing alveolitis: CT–pathologic correlation. *Radiology* 1986;160:585–588.
4. Nishimura K, Kitaichi M, Izumi T, Nagai S, Kanaoka M, Itoh H. Usual interstitial pneumonia: histologic correlation with high-resolution CT. *Radiology* 1992;182:337–342.
5. Johkoh T, Muller NL, Cartier Y, Kavanagh PV, Hartman TE, Akira M, Ichikado K, Ando M, Nakamura H. Idiopathic interstitial pneumonias: diagnostic accuracy of thin-section CT in 129 patients. *Radiology* 1999;211:555–560.
6. MacDonald SL, Rubens MB, Hansell DM, Copley SJ, Desai SR, du Bois RM, Nicholson AG, Colby TV, Wells AU. Nonspecific interstitial pneumonia and usual interstitial pneumonia: comparative appearances at and diagnostic accuracy of thin-section CT. *Radiology* 2001; 221:600–605.
7. Kawamura T, Matsumoto T, Tanaka N, Kido S, Jiang Z, Matsunaga N. Crackle analysis for chest auscultation and comparison with high-resolution CT findings. *Radiat Med* 2003;21:258–266.
8. Raghu G, Mageto YN, Lockhart D, Schmidt RA, Wood DE, Godwin JD. The accuracy of the clinical diagnosis of new-onset idiopathic pulmonary fibrosis and other interstitial lung disease: a prospective study. *Chest* 1999;116:1168–1174.
9. Sumikawa H, Johkoh T, Ichikado K, Taniguchi H, Kondoh Y, Fujimoto K, Tateishi U, Hiramatsu T, Inoue A, Natsag J, *et al.* Usual interstitial pneumonia and chronic idiopathic interstitial pneumonia: analysis of CT appearance in 92 patients. *Radiology* 2006;241:258–266.
10. Kazerooni EA, Martinez FJ, Flint A, Jamadar DA, Gross BH, Spizarny DL, Cascade PN, Whyte RI, Lynch JP III, Toews G. Thin-section CT obtained at 10-mm increments versus limited three-level thin-section CT for idiopathic pulmonary fibrosis: correlation with pathologic scoring. *AJR Am J Roentgenol* 1997;169:977–983.
11. Kim TS, Lee KS, Chung MP, Han J, Park JS, Hwang JH, Kwon OJ, Rhee CH. Nonspecific interstitial pneumonia with fibrosis: high-resolution CT and pathologic findings. *AJR Am J Roentgenol* 1998; 171:1645–1650.
12. Johkoh T, Muller NL, Colby TV, Ichikado K, Taniguchi H, Kondoh Y, Fujimoto K, Kinoshita M, Arakawa H, Yamada H, *et al.* Nonspecific interstitial pneumonia: correlation between thin-section CT findings and pathologic subgroups in 55 patients. *Radiology* 2002;225:199–204.
13. Park JS, Lee KS, Kim JS, Park CS, Suh YL, Choi DL, Kim KJ. Nonspecific interstitial pneumonia with fibrosis: radiographic and CT findings in seven patients. *Radiology* 1995;195:645–648.
14. Hartman TE, Swensen SJ, Hansell DM, Colby TV, Myers JL, Tazelaar HD, Nicholson AG, Wells AU, Ryu JH, Midthun DE, *et al.* Nonspecific interstitial pneumonia: variable appearance at high-resolution chest CT. *Radiology* 2000;217:701–705.
15. Flaherty KR, Travis WD, Colby TV, Toews GB, Kazerooni EA, Gross BH, Jain A, Strawderman RL, Flint A, Lynch JP, *et al.* Histopathologic variability in usual and nonspecific interstitial pneumonias. *Am J Respir Crit Care Med* 2001;164:1722–1727.
16. Katzenstein AL, Zisman DA, Litzky LA, Nguyen BT, Kotloff RM. Usual interstitial pneumonia: histologic study of biopsy and explant specimens. *Am J Surg Pathol* 2002;26:1567–1577.
17. Daniil ZD, Gilchrist FC, Nicholson AG, Hansell DM, Harris J, Colby TV, du Bois RM. A histologic pattern of nonspecific interstitial pneumonia is associated with a better prognosis than usual interstitial pneumonia in patients with cryptogenic fibrosing alveolitis. *Am J Respir Crit Care Med* 1999;160:899–905.
18. Bjoraker JA, Ryu JH, Edwin MK, Myers JL, Tazelaar HD, Schroeder DR, Offord KP. Prognostic significance of histopathologic subsets in idiopathic pulmonary fibrosis. *Am J Respir Crit Care Med* 1998;157: 199–203.
19. Travis WD, Matsui K, Moss J, Ferrans VJ. Idiopathic nonspecific interstitial pneumonia: prognostic significance of cellular and fibrosing patterns: survival comparison with usual interstitial pneumonia and desquamative interstitial pneumonia. *Am J Surg Pathol* 2000;24: 19–33.
20. Flaherty KR, Thwaite EL, Kazerooni EA, Gross BH, Toews GB, Colby TV, Travis WD, Mumford JA, Murray S, Flint A, *et al.* Radiological versus histological diagnosis in UIP and NSIP: survival implications. *Thorax* 2003;58:143–148.
21. Lynch DA, David Godwin J, Safrin S, Starko KM, Hormel P, Brown KK, Raghu G, King TE Jr, Bradford WZ, Schwartz DA, *et al.* High-resolution computed tomography in idiopathic pulmonary fibrosis: diagnosis and prognosis. *Am J Respir Crit Care Med* 2005;172:488–493.